Interfacial photochemistry of marine diatom lipids: Abiotic production of volatile organic compounds and new particle formation

A. Penezic, X. Wang, S. Perrier, C. George, S. Frka

▶ **To cite this version:**

A. Penezic, X. Wang, S. Perrier, C. George, S. Frka. Interfacial photochemistry of marine diatom lipids: Abiotic production of volatile organic compounds and new particle formation. Chemosphere, 2023, 313, 10.1016/j.chemosphere.2022.137510 . hal-03951381

HAL Id: hal-03951381
https://hal.science/hal-03951381v1

Submitted on 12 Oct 2023

HAL is a multi-disciplinary open access archive for the deposit and dissemination of scientific research documents, whether they are published or not. The documents may come from teaching and research institutions in France or abroad, or from public or private research centers.

L'archive ouverte pluridisciplinaire **HAL**, est destinée au dépôt et à la diffusion de documents scientifiques de niveau recherche, publiés ou non, émanant des établissements d'enseignement et de recherche français ou étrangers, des laboratoires publics ou privés.

Interfacial photochemistry of marine diatom lipids: Abiotic production of volatile organic compounds and new particle formation

Abra Penezić*[1], Xinke Wang[2,3], Sebastien Perrier[2], Christian George[2], Sanja Frka*[1]

[1]Division for Marine and Environmental Research, Ruđer Bošković Institute, Zagreb, Croatia
[2]Université Lyon, Université Claude Bernard Lyon 1 CNRS, IRCELYON, Villeurbanne, France
[3]Now at Department of Chemistry, University of California, Irvine, CA 92697-2025
*Corresponding authors: abra@irb.hr; frka@irb.hr

Abstract

The global importance of abiotic oceanic production of volatile organic compounds (VOCs) still presents a source of high uncertainties related to secondary organic aerosol (SOA) formation. A better understanding of the photochemistry occurring at the ocean-atmosphere interface is particularly important in that regard, as it covers > 70% of the Earth's surface. In this work, we focused on the photochemical VOCs production at the air-water interface containing organic material from authentic culture of marine diatom *Chaetoceros pseudocurvisetus*. Abiotic VOCs production upon irradiation of material originating from total phytoplankton culture as well as the fraction containing only dissolved material was monitored by means of PTR-ToF-MS. Furthermore, isolated dissolved lipid fraction was investigated after its deposition at the air-water interface. All samples acted as a source of VOCs, producing saturated oxygenated compounds such as aldehydes and ketones, as well as unsaturated and functionalized compounds. Additionally, a significant increase in surfactant activity following irradiation experiments observed for all samples implied biogenic material photo-transformation at the air-water interface. The highest VOCs flux normalized per gram of carbon originated from lipid material, and the produced VOCs were introduced into an atmospheric simulation chamber, where particle formation was observed after its gas-phase ozonolysis. This work clearly demonstrates abiotic production of VOCs from phytoplankton derived organic material upon irradiation, facilitated by its presence at the air/water interface, with significant potential of affecting the global climate as a precursor of particle formation.

1. Introduction

Unicellular marine microalgae are responsible for approximately half of the global net primary production (Field et al., 1998, Bryant, 2003). One of the ecologically most important groups of phytoplankton are diatoms, ubiquitous across aquatic environments, from tropical to polar regions, and from highly dynamic coastal and upwelling habitats to more stable oceanic waters (Malviya et al., 2016, Bruland et al., 2005), accounting for approximately 20% of the global primary production (Mock and Medlin, 2012). Diatoms thus play a major role in carbon biogeochemical cycles (Field et al., 1998), in part through volatile organic compounds (VOCs) production, as a way of enhancing abiotic stress resistance, transferring information, protecting against predators and playing allelopathic roles (Zuo, 2019).

Major components of diatoms are lipids, accounting for up to 25% of their dry weight (Levitan et al., 2014). Production of lipids in diatom varies depending on culture conditions (Yi et al., 2017), however, diatom lipid material contains nearly all lipid classes, including both polar (Guschina and Harwood, 2006) and neutral lipids, such as free fatty acids (FFA), sterols (ST) and triacylglycerols (TG). Biogenic lipids are integral parts of cellular membranes (digalactosyldiacylglycerol (DGDG), monogalactosyldiacylglycerol (MGDG), sulfoquinovosyldiacylglycerol (SQDG), phosphatidylglycerol (PG) and phosphatidylcholine (PC)) (Stonik and Stonik, 2015) and energy storage molecules (TG), especially during specific environmental conditions such as nutrient starvation (Levitan et al., 2015).

Phytoplankton presents a main source of marine lipids through activities such as direct release, metabolic processes and cell lysis, which then have a significant impact on various processes in the aquatic environment due to their amphiphilic nature and the ability to accumulate at interfaces. As the top millimetre of the sea surface, the sea surface microlayer (SML) represents the largest environmental interface where many important processes such as wind action, water transpiration, solar energy flux and atmospheric interactions take place (Blough, 2005; Wurl et al., 2017). The SML is enriched with surface active organic matter (or surfactants) which accumulates at the air-water interface and forms surface films (Wurl and Holmes, 2008; Wurl et al., 2011; Frka et al., 2009, 2012). Although lipid material presents only a small portion of the organic matter (OM) pool in the SML, its presence at the air-water interface is the result of competitive adsorption and segregation from other macromolecular constituents due to its extremely high surface affinity (Frka et al., 2012). Biogenic lipids are also known to play a role in the formation and stabilization of the SML, as well as the physico-chemical, and morphological properties of the marine surface films (Van Vleet and Williams, 1983). Such

surface films were found to have considerable effects on marine biogeochemical and climate-related mechanisms by directly affecting processes such as exchange of trace gases (e.g., CO_2) (Engel et al., 2017; Milinković et al., 2022; Barthelmeß et al., 2021). Additionally, OM can be emitted directly from the ocean to the atmosphere, constituting the primary marine aerosol (Cochran et al., 2016; Chingin et al., 2018; Frossard et al., 2019) by wind-driven processes and bubble bursting (Facchini et al., 2008; Frossard et al., 2014, 2019). In primary aerosol, organic compounds enriched in the SML have been identified, including surface active dissolved organic matter (DOM) like polymers incorporated into microgels, but also transparent exopolymer particles (TEP) and Coomassie stainable particles (CSP) (Kuznetsova et al., 2005; Orellana et al., 2011; Aller et al., 2017). Long chain saturated fatty acids, such as palmitic acid and stearic acid, corresponding to major constituents of the SML, were also detected in marine aerosols (Marty et al., 1979; Slowey et al., 1962; Wu et al., 2015; Hu et al., 2018; Kang et al., 2017). The transfer and enrichments of the biogenic lipid classes on aerosol particles may be related to the distribution of compounds within the bubble-air-water interface (Triesch et al., 2021, Ellison et al., 1999).

Furthermore, a recent field study by Mungall et al. (2017) reinforced for the first time previous laboratory observations, by hypothesizing that photochemistry at the air-water interface could have a role as a novel source of oxygenated VOCs to the marine boundary layer. These emissions were exclusively attributed to the photochemical reactions facilitated by the presence of surfactants at the air-sea interface. Namely, experimental photosensitized reactions at the air-water interface by using humic acids as a proxy for DOM have led to chemical conversion of linear saturated fatty acids into unsaturated functionalized gas-phase products (Ciuraru et al., 2015a). Also, recent studies showed intensive photochemistry of dimethyl sulfoxide (DMSO) facilitated by polycyclic aromatic hydrocarbons (PAHs), a group of primary pollutants, at the air-water interface, leading to the formation of organosulfur compounds in the gas and the aqueous phases (Jiang et al., 2021., Mekic et al., 2020). Atmospheric photochemistry was even shown to take place in the absence of photosensitizers if the air-water interface is coated with a fatty acid (Rossignol et al., 2016). On a global scale, interfacial photochemistry has recently been suggested to act as an abiotic source of VOCs, comparable to their marine biological emissions (Brüggemann et al., 2018). VOCs have been shown to be important precursors to secondary organic aerosol (SOA) formation. Recent studies revealed that SOA, accounting for as much as 50-85% of the total organic aerosol burden (Jimenez et al., 2009), can strongly impact the radiation balance of the atmosphere, modify cloud

microphysics, and participate in chemical transformations (Zhu et al., 2017). Marine SOA of biogenic origin could be especially important for understanding the cloud-mediated effects of aerosols on climate, because cloud properties respond to aerosols in a nonlinear way and are most sensitive to the addition of particles when the background concentration is low.

Although previous studies have demonstrated photoinduced VOCs production from artificial surfactants in laboratory grade water (Fu et al., 2015; Alpert et al., 2017; Bernard et al., 2016), saline solutions (Ciuraru et al., 2015a), and biofilm-containing solutions comprising a mixture of different microorganisms (Brüggemann et al., 2017), these experiments were typically conducted under far from ambient conditions or for a very limited number of authentic samples (Ciuraru et al., 2015b). To investigate the potentially underestimated VOCs source under more realistic conditions, in this study the biogenic OM was produced from an authentic diatom culture. Additionally, lipid material was isolated to further investigate phytoplankton lipid material as the main driver of surfactant release and, thus, abiotic photochemical VOCs production. Experiments were conducted in a photochemical reactor and an atmospheric simulation chamber, to study VOCs formation upon irradiation and implications for aerosol formation and growth, respectively. An improved chemical characterization of the surface-active organic compounds of marine origin and their interfacial photochemical processing is highly desirable to better understand the abiotic VOCs sources, and to improve our understanding of their subsequent impact on the climate.

2. Methods

2.1. *Chaetoceros pseudocurvisetus* culture and sample preparations

Batch culture of C. pseudocurvisetus (10^5 cells) was inoculated in sterile VWR® Tissue Culture Flasks (VWR, Radnor, Pennsylvania) and placed in a temperature-controlled incubator (20 °C) under illumination of 4500 lx on a 12h/12h light/dark cycle. The growth medium was F/2 medium (Guillard, 1975) with a lowered nitrogen content (NO_3^-: 42 µmol L^{-1}), relevant for nutrient depleted oligotrophic waters, which represent 60% of the global ocean. The media was prepared in North Adriatic seawater rested for 6 months in the dark, filtered through sterile 0.22 µm filters (Merck Millipore Ltd.) and microwave boiled (Keller et al., 1988). Media amendments were added aseptically after sterilization. The cell number was controlled by a Fuchs-Rosenthal Chamber hemocytometer equipped with an Olympus BX51-P polarizing microscope. The growth was terminated on day eight, at the onset of the stationary phase.

At the onset of stationary phase growth (4 x 10^6 cells), an aliquot of the original phytoplankton solution (hereafter, total solution, TS) was immediately frozen and kept at -20 °C until further experiments. Due to cell bursting caused by freezing and defrosting, the TS sample used for experiments contained dead cell material along with the phytoplankton produced dissolved organic matter. Further, in order to obtain only dissolved fraction (DS) of the biogenic sample, an aliquot of the original phytoplankton solution was filtered through a pre-combusted (5 h at 450 °C) 0.7 µm Whatman (Kent, UK) GF/F filter. Following filtration, the DS was immediately frozen and kept at -20 °C until further experiments. Finally, to obtain a sample of dissolved lipid material from TS sample, 200 mL of the original phytoplankton solution filtrate was extracted by liquid-liquid extraction with dichloromethane (LiChrosolv®, Merck), twice at pH 8 and twice at pH 2, following hydrochloric acid addition. Extracts were evaporated until dry by rotary evaporation under a nitrogen atmosphere and stored at -20 °C until measurements. The obtained extracts present the biogenic lipid material sample (LS) further investigated in irradiation experiments. The lipid classes of the extracted material were analyzed by thin layer chromatography after addition of an internal standard, 2-nonadecanone (purity ≥ 97%, Sigma Aldrich) (5 µg). Glassware used for lipid sample preparation was washed with chromic acid and rinsed with ultrapure water (MQ water, Merck Millipore, Burlington, Massachusetts, USA). The detailed procedure can be found elsewhere (Gašparović et al., 2017, 2015).

2.2. Organic matter analysis

2.2.1. Particulate and dissolved organic carbon

For measurements of dissolved (DOC) and particulate (POC) organic carbon concentrations, the culture sample was filtrated through a pre-combusted (5 h at 450 °C) 0.7 µm Whatman GF/F filter. Following filtration, the GF/F filter was stored at −80 °C until POC analysis. DOC analysis aliquots were collected in duplicates in 22 mL glass vials pre-combusted at 450 °C for 4 h. Sample preservation was done with mercury chloride (10 mg L^{-1}) and samples were stored at +4 °C in the dark until analysis. Samples for DOC and POC were analyzed according to methods EN 1484:2002 in a laboratory accredited according to the EN ISO/IEC 17025:2017 standard. A TOC-V_{CPH} analyzer (Shimadzu, Japan) equipped with a platinum silica catalyst and nondispersive infrared (NDIR) detector for CO_2 measurements was used for DOC measurements. Concentration was calculated as an average of 3–5 replicates. The average instrument and MQ water blank were 0.03 mg L^{-1}, with a high reproducibility (1.6%). POC was analyzed with a solid sample module SSM-5000A associated to a Shimadzu TOC-V_{CPH} carbon analyzer calibrated with glucose. To remove inorganic carbonate fraction, filters were

acidified with hydrochloric acid (2 mol L^{-1}), and dried afterwards at 50 °C for 12 h. The samples were incinerated in a flow of oxygen at 900 °C, and the CO_2 produced was detected by an NDIR detector. POC concentrations were corrected based on the blank filter measurements. The average instrument and MQ water blanks correspond to 0.42 μmol L^{-1}. The reproducibility of measurements determined by using a glucose standard was 3%.

2.2.2. Surfactant activity

Phase sensitive alternating current (a.c.) voltammetry (out-of-phase signal, frequency 77 Hz, amplitude 10 mV) was used for the quantification of surface-active substances (SAS) in TS and DS samples before and after irradiation. The concentration of SAS is expressed as the equivalent amount of the selected standard of non-ionic surfactant tetra-octylphenolethoxylate (Triton-X-100; mg L^{-1}) as described in details previously (Ćosović and Vojvodić, 1982, Frka et al., 2009). Electrochemical measurements were performed using 663 VA Stand with potentiostat/galvanostat μAutolab II and automatic Hg drop production (Metrohm Autolab B.V., The Netherlands) equipped with GPES 4.9 software (Eco Chemie B. V., Uttrecht, The Netherlands). An automated hanging mercury drop electrode (HMDE, Metrohm, Switzerland) was used as a working electrode, Ag/AgCl/3 mol L^{-1} KCl as the reference electrode and a Pt coil as the auxiliary electrode. SAS measurements of the LS samples before and after irradiation were performed by re-dissolving the dry lipid aliquot in 0.55 mol L^{-1} NaCl (Suprapur®, Merck, Germany) as the supporting electrolyte (see 2.3.2. Aqueous Phase analysis).

2.2.3. Lipid classes

Aliquots of the lipid extracts re-dissolved in dichloromethane were spotted onto silica-coated quartz thin-layer chromatography rods, where they were developed in a series of seven developing baths containing mixtures organic solvents of increasing polarity. Eighteen lipid classes were separated and analyzed by thin–layer chromatography flame ionization detection (TLC–FID) (Iatroscan MK–VI, Iatron, Japan), at a hydrogen flow of 160 mL min^{-1} and air flow of 2000 ml min^{-1}, and quantified by external calibration with a standard lipid mixture. More experimental details can be found in Gašparović et al (2015, 2017). Limits of detection (LODs) were determined as the analyte concentrations corresponding to a signal-to-noise (S/N) ratio of 3. The sample was analysed in triplicate. Total lipid concentration was determined as a sum of all quantified lipid classes: sterol esters (SE); fatty acid methyl esters (ME); fatty ketone hexadecanone (KET, internal standard); triacylglycerols (TG); free fatty acids (FFA);

fatty alcohols (ALC); 1,3-diacylglycerols (1,3 DG); sterols (ST); 1,2-diacylglycerols (1,2 DG); pigments (PIG); monoacylglycerols (MG); three classes of glycolipids (GL): mono- and di-galactosyldiacylglycerols (MGDG and DGDG) and sulfoquinovosyldiacylglycerols (SQDG), and three classes of phospholipids (PL): phosphatidylglycerols (PG), phosphatidylethanolamines (PE), and phosphatidylcholine (PC).

2.2.4. Chlorophyll *a*

Subsamples (500 mL) for the determination of chlorophyll *a* (Chl *a*) were filtered on 0.7 μm Whatman GF/F glass filters and stored at −20 °C until further processing. Spectrometric determination of the Chl *a* concentration was determined according to ISO 10260:1992 method with minor modifications. Samples were extracted in 95% ethanol (10 mL) at 60 °C for 1 h in dark, centrifugated (Rotofix 32A, Hettich) for 10 min at 4000 rpm and absorbance was measured on a Turner TD-700 spectrophotometer at 750 nm and 665 nm before and after the addition of 10 μL 2 mol L^{-1} HCl.

2.3. Photochemical reactor experiments

Phytoplankton culture samples TS and DS (7 mL) were placed into an acid cleaned circular borosilicate glass reactor cell (height 4 cm, inner diameter 5 cm, volume 80 cm^3), thermostated to 20 °C, and mounted with a Quartz window. The experiment with the lipid sample (LS) was conducted by spreading the hexane lipid extract aliquots, with a syringe (Hamilton, Nevada, USA), on the surface of a seawater model solution (0.55 M NaCl), to correspond to the ionic strength of the two other samples (TS and DS). The system was left for 15 min under very slow flow, in order for the hexane to evaporate, obtaining in this way a lipid film at the air-water interface. The surplus of lipid material is added to ensure a fully covered surface (near-monolayer coverage) due to losses on the cell walls. A Xenon lamp (150 W; LOT Quantum Design, France) placed at a distance of 13 cm from the reactor was used to mimic solar irradiation on the Earth's surface (**Figure S1**). A quartz water filter of 5 cm was mounted in front of the lamp to remove infrared irradiation, while short wavelengths ($\lambda < 290$ nm) were eliminated by a Pyrex filter positioned directly in front of the reactor. A flow of 200 – 300 mL min^{-1} of compressed, filtered and purified air was pushed continuously through the reactor. Typically, after the introduction of the samples and acquisition of a stable background signal, the samples were irradiated for 1 h. Irradiation measurements were replicated, and only their typical time profiles were presented herein. Experiments were stopped when signals reached background levels again, after switching off the light. All experiments were preceded by

background VOCs experiments performed on an empty reactor containing ultrapure water. The values of SAS in blank samples (MQ water that was placed in the reactor) were as below limit of quantification (0.02 mg L^{-1} eq. T-X-100). It should be noted that temperature effect can be excluded in our experiments as temperature control tests have been performed. Concentrations of VOCs were calculated according to Cappellin et al. (2012) and expressed as ppbv. VOCs fluxes (molecule cm^{-2} s^{-1}) were calculated according to Equation 1 (Ciuraru et al. (2015b)):

$$F = C \times Q / S \times L$$

where C is the concentration of the detected compound (molecules cm^{-3}), Q is the flow rate of air into the cell (cm^3 s^{-1}), S is the surface area of the solution (cm^2) and L is the light intensity (mW cm^{-2}). Light intensity of the Xe lamp, assuming that only the UV-A fraction is responsible for the observed photochemistry, was 8 mW cm^{-2} for wavelengths below 400 nm. The mean solar flux used was 21 mW cm^{-2}. To obtain normalized fluxes molecule cm^{-2} s^{-1} gC^{-1} the obtained VOC flux values were divided by the weight of carbon in the respective samples.

2.3.1. Gas Phase analysis

A selected reagent ion-proton transfer reaction-time-of-fight mass spectrometer (SRI-PTR-ToF-MS 8000, Ionicon Analytik GmbH, Innsbruck, Austria) was used to quantify the emitted VOCs using H_3O^+ as source reagent ions. More details about the setup and calibration of the PTR-MS were described in a previous study (Kalalian et al., 2020). Briefly, air was sampled at a constant flow of 50 ml min^{-1} at an inlet temperature of 333 K. Typically, a drift voltage of 550 V, a drift temperature of 353 K and a drift pressure of 2.2 mbar were used, resulting in an E/N-ratio of about 135 Td.

2.3.2. Aqueous Phase analysis

Immediately after irradiation experiments TS and DS sample aliquots were frozen at -20 °C for further DOC and surfactant analyses (described above). An aliquot of irradiated LS sample was extracted twice with dichloromethane. Extract was evaporated to dryness by rotary evaporation under a nitrogen atmosphere and stored at −20 °C until SAS measurements.

2.4. Atmospheric simulation chamber

Particle formation upon oxidation of the VOCs originating from the LS sample was investigated using a 2 m^3 chamber made of fluorinated ethylene propylene (FEP) film. The chamber was surrounded by 12 UV-Vis lamps (OSRAM lamps, Eversun L80W/79-R) to mimic solar irradiation. When all chamber background levels were established, the filling of the

chamber with VOCs produced from LS sample irradiation in quartz reactor cell was conducted. After 48 h of filling, the ozone, generated by UV photolysis of oxygen (Stable Ozone Generator 1, Ultra-Violet Products Ltd., USA), was injected in the dark, reaching a maximum of 300 ppbv. The initial chamber temperature, humidity and air pressure were 30 °C, 7.7% and 1.3 Pa, respectively. Chamber conditions were monitored throughout the experiment (**Figure S2**). Gas-phase concentration of VOCs was monitored with a PTR-ToF-MS using H_3O^+ as source reagent ions. The resulting O_3 concentrations in the chamber were continuously monitored by Ozone Analyser (49i, Thermo Scientific, USA). Particle number concentrations and corresponding size distributions were measured using an ultrafine condensation particle counter (UCPC, 3776, TSI, USA) and a scanning mobility particle sizer (SMPS, 3936, TSI, USA). The chamber is continuously slightly over pressurized to avoid any possible contamination of ambient lab air. For this purpose, a flux of pure air compensates the air withdrawn by the different analytical instrument connected to the chamber. After the particle concentrations reached an approximate steady state concentration, the UV lamps were turned on for 1 h to further study SOA ageing.

3. Results and discussion

3.1. Initial characteristics of phytoplankton culture sample

At the onset of the stationary growth phase, the concentrations of POC, DOC, Chl *a*, dissolved lipids, and lipid carbon content of the dissolved fractions of the phytoplankton culture sample were determined and results are presented in **Table 1**.

Table 1. Initial properties of phytoplankton culture sample.

Chl *a* mg L^{-1}	DOC mg L^{-1}	POC mg L^{-1}	DLip mg L^{-1}	DLipC mg L^{-1}
25.9±3.1	2.9±0.1	6.2±0.2	1.2±0.1	0.8±0.1

The high POC concentration of 6.2 mg L^{-1} is due to abundant cell content (4 x 10^6 cells), which is also evident from the high Chl *a* concentration of 25.9 μg L^{-1}. Obtained DOC and POC concentrations were within the range of mean values typically detected in the sea surface microlayer of Adriatic Sea coastal area (DOC 1.5 mg L^{-1} and POC 3.5 mg L^{-1}) (Milinković et al., 2022). Marine lipids are an important component of marine OM (Frka et al., 2011), with

the dissolved fraction (DLip) originating from: primary production and release during life cycle, after cell death, or from dissolution of the particulate fraction (Yoshimura et al., 2009; Novak et al., 2018). Marić et al. (2013) reported that dissolved lipids in the northern Adriatic Sea ranged from 10.3 to 70.6 μg L^{-1}, and were dominated by glycolipids, phospholipids and free fatty acids. Increased sea temperatures facilitate marine DOC and DLip production, with more pronounced effects under nutrient limiting conditions (Novak et al., 2019, 2018). The amount of carbon in the extracted LS (**Table 1**) was determined based on the assumption that lipid carbon accounts for 70% of total lipid concentration (Novak et al., 2018). The contribution of DLip to DOC in the phytoplankton culture sample was approximately 28%, which is in accordance with similar phytoplankton growth studies (e.g. Novak et al., 2018). Dissolved lipid material was dominantly composed of polar lipids, i.e., phospholipids (PL) and glycolipids (GL) (**Figure 1**). The two groups accounted for 35 ± 6% and 21 ± 3% of the total DLip, respectively. Phosphatidylglycerols (PG) dominated within PL while monoacylglycerols (MDGD) contributed the most to GL. Dissolved PL are assumed to be a part of the non-living organic matter released from phytoplankton cells upon cell death since PL are essential components of membranes where they share a structural function with sterols. In algae and cyanobacteria, like in higher plants, GL are located predominantly in the photosynthetic membranes (thylakoids), where they are the most abundant type of lipids (Guschina and Harwood, 2009). It was found that phytoplankton adapted to low nutrient conditions enhanced MGDG synthesis because these molecules do not contain nitrogen or phosphorus (Frka et al., 2011). The most common glycolipids in plankton are MGDG, digalactosyldiacylglycerols (DGDG) and sulfoquinovosyldiacylglycerol (SQDG) although mannose, glucose and glucuronic acid are also found as constituent sugars in GL (Guschina and Harwood, 2009). High abundance of MGDG and PG indicates dominance of freshly produced OM, while the non-living material signifies the more re-worked lipid degradation indices (FFA, MG, 1,2- and 1,3-DG). FFA as indicators of lipid material degradation accounted for 12 ± 2% of lipids, while remaining lipid classes contributed by only 7% or less.

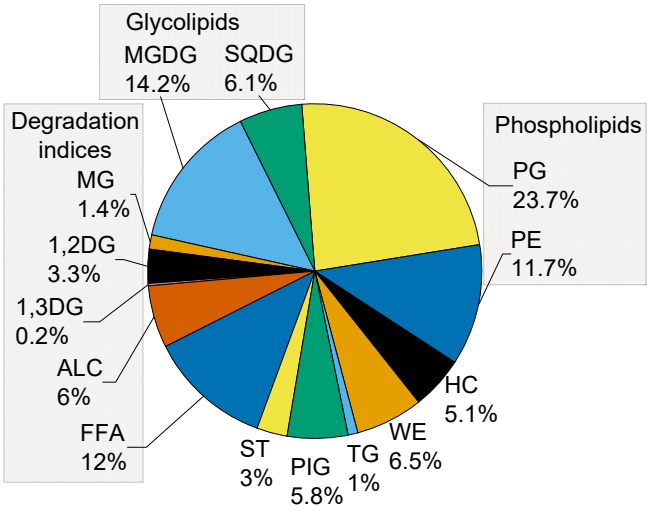

Figure 1. The composition of lipid classes in the dissolved fraction of *C. pseudocurvisetus* culture sample.

3.2. Photochemical transformation of biogenic material and VOCs production

Upon irradiation of biogenic material present in the three different fractions originating of the same phytoplankton culture sample, rapid VOCs release was detected. Since all samples contained only non-living material, direct biological mechanisms can be assumed to have had no effect on the VOCs production, meaning that all VOCs were formed through abiotic photochemical reactions. The total VOCs fluxes normalized per gram of carbon for TS, DS and LS samples are shown in **Figure 2**. Higher normalized VOCs emission flux measured in TS compared to DS shows that particulate material from the dead cells present in TS may be responsible for the enhanced release of VOCs precursors in addition to the dissolved biogenic material. This is consistent with previous findings showing that lysis of riverine microbial cells due to cell death was a significant source of surfactant compounds acting as VOC precursors (Brüggemann et al., 2017). Indeed, particles have a role in facilitating the accumulation and transport of surface active material, including lipid material, to the ocean-atmosphere interface. Therefore, the enrichment of the particulate organic fraction in the sea surface microlayer is typically greater than the enrichment of the dissolved fraction (Marty et al., 1988; Kuznetsova and Lee, 2002; Kuznetsova et al., 2005; Burrows et al., 2014, Milinković et al., 2022).

The highest normalized flux intensity was obtained for the LS sample. This implies that biogenic lipid material completely distributed at the air-water interface and forming a surface film, is primarily responsible for the photochemical reactions leading to the production of VOCs from diatom OM during irradiation. Since the LS lipids present a fraction of the DS and

TS organic material, we can assume that due to experimental conditions (insufficient time, no bubbling or stirring), lipid material from bulk of TS and especially of DS, did not accumulate sufficiently at the air-water interface to form more closely packed surface films and enable more intense VOC production. Indeed, the experiment with LS being directly spread on the air-water interface, represents the ultimate (endpoint) situation, assuming that surface active/hydrophobic SAS fraction of the biogenic sample completely accumulates on the air-water surface and forms a condensed monolayer. The study by Ciuraru et al. (2015a) also showed that VOC concentrations levelled off when the surface tension of the model nonanoic fatty acid decreased due to the dense packing of the surface monolayer at the air-water interface. It was previously observed that the presence of lipids at the ocean-atmosphere interface, i.e. the sea surface microlayer, is the result of its competitive adsorption and segregation from other macromolecular constituents (Frka et al., 2012), and that the formation of a lipid surface film, as well as its properties, are strongly affected by other organic material present (Kozarac et al., 2000).

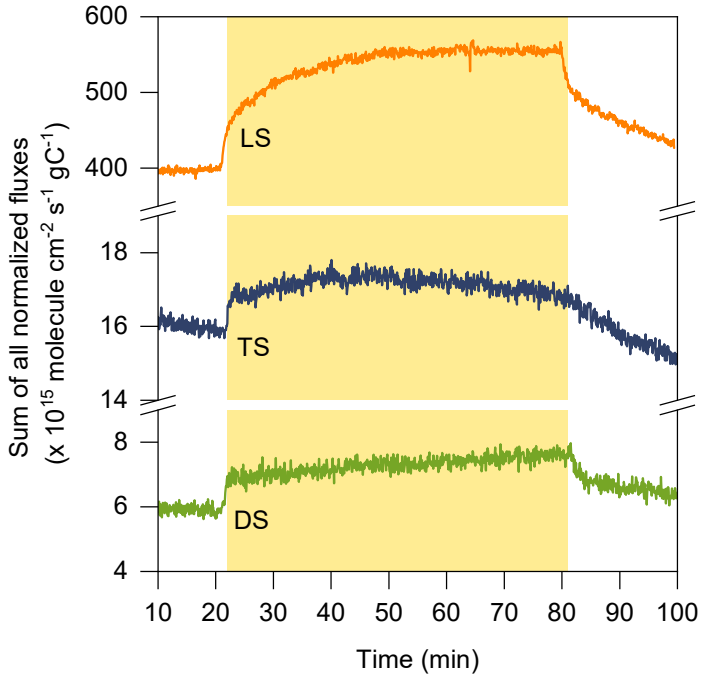

Figure 2. VOC fluxes in TS, DS and LS normalized per gram of carbon. Yellow color represents the period of irradiation.

Photochemical processing of the three samples exposed to light was followed by comparing their surfactant activity before and after irradiation (**Figure 3**). As observed, irradiation induced

a significant increase in the surface activity of the organic material present in TS, DS and LS samples. An increase in surface activity upon irradiation of the SML and underlying water was recently reported by Rickard et al. (2022), showing that in addition to temperature, which is known to affect surfactant adsorption kinetics, irradiation independently contributes to enhanced interfacial surfactant activity due to photo-degradation of larger organic molecules. The less water-soluble substances i.e., surfactants present in the bulk of the TS and DS samples might spontaneously accumulate at the air-water interface and drive the observed photo-induced VOCs production. Furthermore, our results confirmed photo-induced increase of OM surface activity, which additionally facilitated OM accumulation at the air-water interface and further simultaneous formation of the detected VOCs.

The highest normalized flux intensity originated from the LS sample, also characterized by the highest surface activity, pointing to the importance of the photochemical processing of biogenic lipids as efficient surfactants in the VOCs formation in the marine environment.

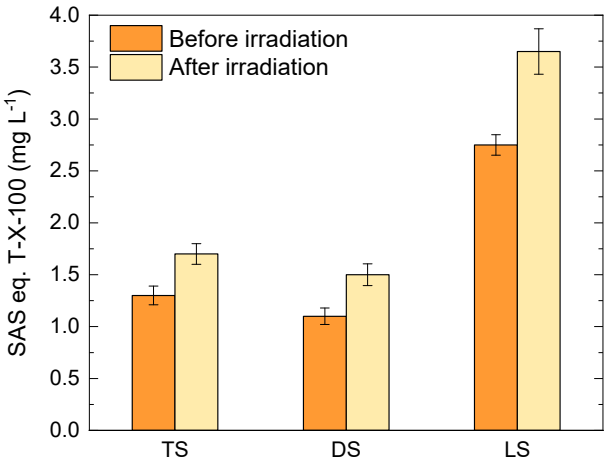

Figure 3. Surface activity of TS, DS and LS samples measured before and after irradiation.

The notion of omnipresence of aerosol bound surfactants from ocean waters has been supported by recent laboratory studies linking aerosol production and fatty acid composition with marine biological activity (Alpert et al., 2015, 2017, Cochran et al., 2016). This is especially relevant because surfactants on water aerosol particles and droplets may undergo unique photochemical reactions upon irradiation (Rossignol et al., 2016, George et al., 2015), due to distinctly different physical and chemical properties of interfaces, compared to bulk and gas phases.

Another driving force of photochemical reactions includes photosensitizers. TS and DS contained photosensitizing organic molecules, as well as traces of photo-active transition metals such as Fe and Cu, which could have additionally initiated the observed photochemistry (Huang et al., 2020). Photosensitized reactions were also possible in the LS sample, where pigments that could act as photosensitizers, accounted for 5 ± 3% of the total lipids (**Figure 1**). More specifically, chlorophylls are very efficient photosensitizers under both photosynthetic active radiation (PAR) (Nelson, 1993) and ultraviolet radiation (UVR) (He and Häder, 2002) since they absorb in the UVR range (Quesada and Vincent, 1997; Ehling-Schulz and Scherer, 1999) and enable type II (i.e. involving singlet oxygen) oxidation processes (Rontani, 2001). Christodoulou et al. (2010) showed that photodegradation of most of the unsaturated lipids of E. huxleyi cells (chlorophylls, sterols and monounsaturated fatty acids) involved type II photosensitized processes, induced by both UVR and PAR. UVR exposure also induced photosensitized stereomutation (*cis-trans* isomerization) of double bonds of some lipids, leading to the production of compounds sufficiently specific to act as tracers of UVR-induced photodegradation in the natural environment.

A decrease in VOCs concentration was observed prior to irradiation in TS sample, indicating a potential removal of gaseous compounds present, as the stream of air is flushing the area above the sample and introducing it into the PTR-ToF-MS. The potential de-gassing of the TS sample was particularly related to C_3H_6O (*m/z* = 59.048), attributable to acetone, which dominated the total VOCs flux, and whose concentration decreased prior to irradiation was followed by an immediate increase when irradiation started, which continued to increase for a while, before again showing a decreasing trend (**Figure S3).** C_3H_6O was not detected in DS, as particulate material producing it in TS might have been removed during the filtration of the sample. C_3H_6O formed from LS exhibited different behaviour compared to TS, indicating different processes or material present were responsible for C_3H_6O formation in different types of biogenic samples. Thus, constant concentrations prior to irradiation were followed by a gradual increase upon irradiation (**Figure S3**) indicating continuous production of C_3H_6O by abiotic processes originating from lipid material present at the air-water interface. Along with C_3H_6O, saturated oxygenated VOCs, such as aldehydes and ketones, as well as unsaturated and functionalized VOCs (e.g., alkenes, dienes, unsaturated aldehydes or ketones) were photochemically produced from the analysed samples (**Table 2**). Thus, C_3H_4O, attributable to acetaldehyde, dominated the VOCs flux originating from DS and LS samples. Most of the VOCs were previously observed in photochemical studies of marine SML and biofilm samples

and surfactant-containing aqueous solutions, and attributed to photochemistry at the air-water interface - photosensitized reactions as well as photo-activity of organic surfactants without the presence of photosensitizers (Brüggemann et al., 2017; Rossignol et al., 2016; Ciuraru et al., 2015a, 2015b; Chiu et al., 2017). Photochemical activity and VOCs production thus occur in an organic-enriched environment, typically found at the air-water interface of surfactant-containing aqueous solutions.

The highest number of VOCs originated from the LS (**Table 2**), where along with C_3H_6O, C_2H_4O (*m/z* = 45.033) and CH_4O (*m/z* = 33.033), attributable to acetaldehyde and methanol, respectively, significantly contributed to oxygenated VOC fluxes. These compounds are ubiquitous in the atmosphere, affecting the ozone budget of the troposphere, acting as precursors to peroxy acetyl nitrate and presenting significant sinks for hydroxyl radical and the oxidizing capacity of the lower atmosphere, especially in remote marine areas (Lewis et al., 2005; Singh et al., 1995). Photochemical processes, including photodegradation of chromophoric dissolved organic matter (CDOM) are responsible for the formation of acetaldehyde and acetone (Brüggemann et al., 2017; Mopper and Stahovec, 1986; Zhou and Mopper, 1997), with estimations in coastal upwelling locations ranging between 16% and 68% for acetaldehyde and 48 - 100% for acetone, whose production was shown to be higher in light conditions (Dixon et al., 2013). On the other hand, photochemical production of methanol is considered insignificant and mostly of biological origin, based on measurements and modelling (Beale et al., 2015; J. L. Dixon et al., 2011a; Dixon et al., 2011b; Millet et al., 2008; Mincer and Aicher, 2016). However, our data indicate that alongside C_2H_4O (acetaldehyde) and C_3H_6O (acetone), phytoplankton derived lipid material present at the air-water interface could also be a source of photochemically produced CH_4O (methanol). Formation of several other aldehydes was also observed during the irradiation of LS, namely CH_2O (*m/z* = 31.018), C_4H_8O (*m/z* = 73.063) and $C_6H_{12}O$ (*m/z* =101.096), attributable to formaldehyde, butanal and hexanal respectively. Kieber et al. (1997) observed aldehydes in fatty acid/triglyceride-containing seawater samples exposed to sunlight, attributing their origin to photooxidation of linoleic acid and trilinolein. Photooxidation rate for the unsaturated fatty acid and triglyceride was determined to be over 10 times greater compared to the mono- unsaturated species, while photodegradation of e.g. palmitic acids was considered negligible - potentially due to its low concentration at the air-water interface (experimental details do not mention whether or not an interface was present). According to Zhou et al. (2014), the heterogeneous reaction of linoleic acid with O_3 produces n-hexanal ($C_6H_{12}O$) and 3-nonenal ($C_9H_{16}O$), which is then degraded to

malondialdehyde ($C_3H_4O_2$) and further to glyoxal ($C_4H_2O_2$). $C_6H_{12}O$, $C_9H_{16}O$ and $C_3H_4O_2$, detected during the irradiation of LS, indicate that these highly reactive dicarbonyls might potentially originate as secondary products from *C. pseudocurvisetus* fatty acid photodegradation, as FFA present 12% of lipid material of LS samples. FFA are often found as one of the dominant lipid classes in dissolved lipid fraction, and are considered breakdown indices (Novak et al., 2018; Penezić et al., 2010). It is important to note that fatty acids (including mono and polyunsaturated fatty acids) are building blocks of phospholipids and glycolipids, lipid classes that make up 56 ± 3.2% of the total lipids in the LS. Considering that unsaturated fatty acids are especially susceptible to photooxidation (Heath and Packer, 1986, Rontani and Belt, 2020), it is likely that these classes could contribute to the observed VOC production, although detailed studies of VOC production by specific lipid classes are necessary.

C_5H_8 (m/z = 69.069) was detected upon irradiation of all samples examined, and can be potentially attributed to isoprene, bearing in mind all possible interferences as well as potential fragmentations of higher molecular weight compounds (Warneke et al., 2003; Buhr et al., 2002). This assignment was made with respect to our previous work where different analytical tools were used (Ciuraru et al., 2015b). Isoprene has been determined in marine air across the world's oceans (Yu and Li, 2021 and references therein), and although its terrestrial production (400–750 TgC yr^{-1}) exceeds the marine one (0.1–1.9 TgC yr^{-1}) (Arnold et al., 2009; Palmer and Shaw, 2005, Arneth et al., 2008; Guenther et al., 2006, 2012; Carslaw et al., 2000), isoprene of marine origin has a significant impact on SOA formation, especially during phytoplankton blooms in remote oceans (Hu et al., 2013). This is due to isoprene relatively short atmospheric lifetime (approximately 30 min – 1 hour), making its transport from terrestrial sources to marine areas insignificant. In coastal areas of the eastern Mediterranean, an increase in the concentration of isoprene and other VOCs has been observed during the daytime and with increasing temperature (Kameyama et al., 2014, Dayan et al., 2020), suggesting both biological and abiotic photochemical processes involvement. C_5H_8 fluxes during irradiation of phytoplankton-produced OM in this study were on average 8.0 x 10^9 molecule $cm^{-2}s^{-1}$ for the TS sample and 4.3 x 10^9 molecule $cm^{-2}s^{-1}$ for the DS sample. The C_5H_8 flux from the LS sample was the highest observed, and showed a constant increase upon being irradiated, from 10 x 10^9 molecule $cm^{-2}s^{-1}$ to 22 x 10^9 molecule $cm^{-2}s^{-1}$, with an average of 20 x 10^9 molecule $cm^{-2}s^{-1}$ during irradiation. In-situ measured isoprene fluxes ranged between 0.017 – 6 x 10^9 molecule $cm^{-2}s^{-1}$ (Shaw et al., 2010), while an authentic SML sample

studied in laboratory conditions produced isoprene in the range between 7 – 230 x 10^9 molecule $cm^{-2}s^{-1}$ (Ciuraru et al., 2015b). Additionally, studies showed that biotic isoprene production rate by different diatom species can range between 1.12 – 28.48 μmol (g Chl a)$^{-1}$ day^{-1} (Booge et al., 2016 and references therein), which is close to the average C_5H_8 production rate of 33 ± 3 μmol g $Chla^{-1}$ day^{-1}, obtained in our study for the TS sample. As the VOCs production in our samples can be considered exclusively abiotic, these results indicate the significant contribution of the biogenic lipid film processing to the overall isoprene production in the marine environment.

Along with C_5H_8, $C_{10}H_{16}$ (*m/z* = 137.129), attributable to another terpene, was detected originating from the LS sample. Monoterpenes, whose environmental concentrations are lower than those of isoprene, can have a disproportionately significant impact on marine aerosol, due to the higher yield of SOA (Yu and Li, 2021). Reaction of monoterpenes with molecular oxygen, ozone, hydroxyl radicals, NO_x species and chlorine atoms leads to their atmospheric transformation to condensed-phase carbonyls, alcohols, esters, halogenated hydrocarbons and peroxynitrites within hours (Marmulla and Harder, 2014). It was experimentally observed that α-pinene and β-pinene had a SOA yield of 32% and 41% respectively (Luo and Yu, 2010; Yu, 2018), however their significance, especially considering abiotic processes for the global SOA production needs to be studied further (Yu and Li, 2021, Spracklen et al., 2008). Furthermore, $C_2H_4O_2$ (*m/z* = 61.027) and $C_4H_6O_2$ (*m/z* = 87.042), attributable to acetic and methacrylic acid, respectively, were also detected during LS sample irradiation, potentially due to monoterpene oxidation in the presence of OH radicals (Friedman and Farmer, 2018), which could have been formed by direct dissociation with C9 aldehydes (Rossignol et al., 2016).

Table 2. Detected VOCs originating from TS, LS and DS samples with their corresponding normalized fluxes. The en dash (–) signifies that a compound was not detected.

(*m/z*), assigned molecular formula	TS	DS	LS	(*m/z*), assigned molecular formula	TS	DS	LS
	(x 10^{15} molecule cm^{-2} s^{-1} gC^{-1})				(x 10^{15} molecule cm^{-2} s^{-1} gC^{-1})		
(31.018) CH_2O	–	–	1.24	(57.069) C_4H_8	–	0.58	21.81
(47.012) CH_2O_2	–	–	–	(73.063) C_4H_8O	–	–	3.45
(46.028) CH_3NO	–	–	–	(71.083) C_5H_{10}	0.04	–	7.18
(33.033) CH_4O	–	–	9.01	(87.077) $C_5H_{10}O$	–	–	3.04
(43.017) C_2H_2O	–	–	6.47	(69.069) C_5H_8	0.08	0.21	3.85
(42.032) C_2H_3N	–	–	–	(85.063) C_5H_8O	0.05	–	5.95

(44.012) C_2H_3O	–	–	–	(101.056) $C_5H_8O_2$	0.03	–	–
(45.033) C_2H_4O	0.60	4.37	31.67	(81.067) C_6H_8	0.08	–	1.79
(61.027) $C_2H_4O_2$	–	–	3.97	(83.083) C_6H_{10}	0.04	–	2.33
(60.049) C_2H_5NO	–	–	7.98	(85.099) C_6H_{12}	–	–	5.25
(63.040) $C_2H_6O_2$	–	–	0.71	(97.063) C_6H_8O	–	–	0.45
(41.038) C_3H_4	0.12	0.37	8.38	(99.078) $C_6H_{10}O$	0.04	–	1.88
(57.034) C_3H_4O	–	–	1.54	(101.096) $C_6H_{12}O$	–	–	1.21
(73.027) $C_3H_4O_2$	–	–	0.75	(97.099) C_7H_{12}	–	–	2.25
(43.054) C_3H_6	0.20	0.53	16.02	(109.065) C_7H_8O	0.02	–	–
(59.048) C_3H_6O	14.90	–	228.74	(111.077) $C_7H_{10}O$	–	–	0.50
(75.042) $C_3H_6O_2$	–	–	–	(111.115) C_8H_{14}	–	–	1.57
(58.072) C_3H_7N	–	–	1.35	(127.1100 $C_8H_{14}O$	–	–	0.84
(101.021) $C_4H_4O_3$	–	–	–	(141.124) $C_9H_{16}O$	–	–	1.85
(54.046) C_4H_6	0.09	–	–	(137.129) $C_{10}H_{16}$	–	–	1.29
(71.047) C_4H_6O	0.04	–	1.90	(151.107) $C_{10}H_{14}O$	0.02	–	–
(87.042) $C_4H_6O_2$	–	–	0.90	(155.140) $C_{10}H_{18}O$	–	–	1.87

3.3. Atmospheric simulation chamber experiment

The highest concentration and number of produced VOCs was observed during irradiation of LS sample, leading to further investigation of the impact of biogenic lipids on the atmosphere's oxidation potential, aerosol particle formation and growth. LS sample was irradiated within the photochemical reactor for a period of 48 h, during which the produced VOCs were directly introduced into a dark atmospheric simulation chamber. After 48 h, the irradiation was stopped and VOCs in the chamber were analysed by PTR-ToF-MS, revealing a smaller number of compounds (**Table S1**) compared to those previously determined in the LS sample. This is possibly due to wall losses as well as chemical reactions that took place during the filling of the chamber, reducing the number of compounds and leading to the formation of new ones such as CH_2O_2, CH_3NO, C_2H_3N, C_2H_3O, $C_3H_6O_2$, $C_4H_4O_3$, C_4H_8O, $C_5H_8O_2$. An additional reason could also be a dilution from the reactor cell to the chamber, leading to concentrations below the detection limit of PTR-ToF-MS.

Following introduction of ozone, a sharp increase of several VOCs was observed (**Figure 4a**), most pronounced for C_2H_4O (acetaldehyde) and C_3H_6O (acetone), likely due to ozonolysis of organic unsaturated compounds (Conrad et al., 2021; Deng et al., 2018; Millet et al., 2010; Singh et al., 1994). The reaction between ozone and unsaturated organic compounds allows cleavage of unsaturated carbon bonds, facilitating formation of a carbonyl component and a carbonyl oxide as one of Criegee intermediates, and even carboxylic acids (Hammes et al.,

2018; Wegener et al., 2007). The Criegee intermediates formed by ozonolysis are oxidative species (Conrad et al., 2021) which react, among others, with organic acids in the atmosphere, leading to formation of secondary organic aerosols (Chhantyal-Pun et al., 2018). Following O_3 introduction, a potential increase in reactive Criegee intermediates could have caused different reactions among the already present and the newly produced VOCs, leading to significant particle formation within approximately 40 min after a maximum O_3 concentration of around 300 ppbv was reached (**Figure 4b**).

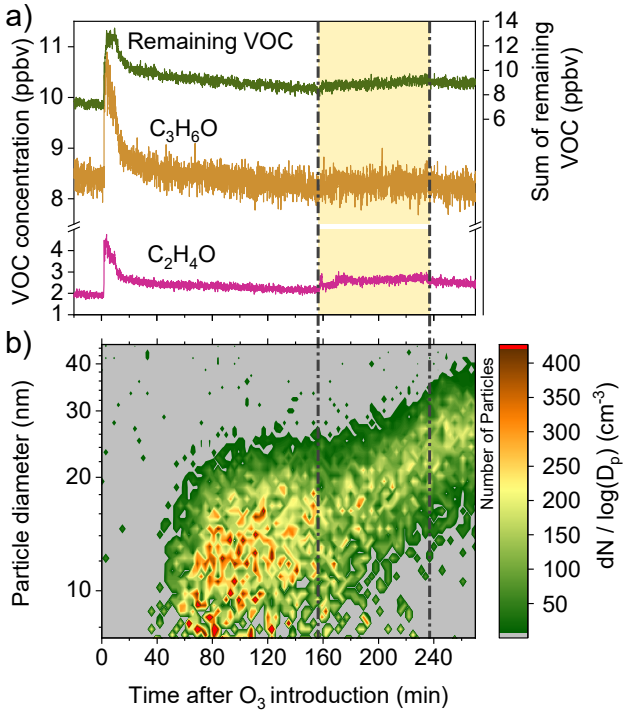

Figure 4. Concentration of C_2H_4O, C_3H_6O, and the sum of all the other detected volatile organic compounds (remaining VOC) in the multiphase atmospheric simulation chamber originating from the dissolved lipid sample at the air-water interface, with irradiation period indicated by the yellow color (a) and the size distribution and number of particles formed within the chamber (b).

A steady increase in particle numbers continued for another 40 min, reaching maximum values. After an initial growth phase when small-sized particles with a diameter of around 10 nm were observed, larger particles began to form, reaching average diameters of around 25 nm (**Figure S4**). According to previous studies, the formation of such small and stable aerosol particles possibly indicated the formation of very stable and low volatile acid–base clusters, or even reaction products (Tang et al., 2013; Qiu et al., 2013; Duporté et al., 2016). This is further supported by the fact that nitrogen-containing compounds are among the VOCs produced and

may act as bases in such reactions (**Table S1**). To study the effect of OH-oxidation and SOA aging, UV lights were turned on after 160 min, and an immediate particle growth was observed (**Figure 4b**). The UV light facilitated the oxidation of the yet unreacted VOCs as well as further low-volatile compound formations, which condensed on the already existing particles, causing particles to increase in size.

3.4. Environmental relevance

In this study we showed that biogenic lipids of phytoplankton origin, as highly surface-active compounds present at the air-water surface, could be exclusively responsible for the photochemical production of VOCs in the marine atmosphere. The VOCs fluxes determined from the lipid sample were within the range of previous field observations and laboratory experiments, suggesting that the observed processes could occur to a similar extent in the marine environment, particularly within the SML directly exposed to the sunlight. It should be noted that such VOCs emissions have previously been attributed to processes driven by biology, artificial surfactants in the laboratory, and biofilm-containing solutions with different microorganisms. In contrast, the observed results suggest that VOCs released during irradiation of exclusively biogenic lipid material of phytoplankton origin accumulated at the ocean-atmosphere interface might lead to similar emissions of saturated and unsaturated VOCs and SOA precursors, impacting atmospheric budgets of cloud condensation nuclei, especially important in clean marine environments. On the other hand, the injection of surfactant films present at the sea-atmosphere interface into the atmosphere in an enriched form as part of the marine aerosol produced by bursting bubbles could occur in real marine conditions. This provides a mechanism for selective transfer of biogenic fatty acids and other marine lipids from the sea to the atmosphere, where photochemistry occurring on the surface of marine aerosol particles may also be a source of VOCs as well as SOA precursors, which could help close the gap for calculating organic aerosol concentrations which are consistently being under-predicted in marine environments. Moreover, such atmospheric processing could result in a change of aerosol surfactant content, directly affecting cloud activation and droplet number, especially important in clean marine atmosphere (Kroflič et al, 2018). There is also increased evidence of the importance of biogenic surfactant films in the air-sea exchange of climate-active gases. The viscoelastic behavior of the air-sea interface, a key parameter affecting air-sea exchange of gases is strongly dependent on naturally occurring adsorbed surfactant material. Namely, natural surfactant films reduce the air-sea gas transfer velocity (k_w) of CO_2 and other gases by up to 50% (Frew, 2005; Salter et al., 2011; Pereira et. al., 2016; 2018; Milinković et al 2022),

and photochemical changes to lipid-like surfactant material can modify k_w, as well as marine boundary layer chemistry.

As a consequence of anthropogenic activity and climate change, many properties of the oceanic environment are changing rapidly. Phytoplankton as a primary producer is highly dependent on changing environmental conditions because of its adaptive evolution strategies aimed at survival. Important adaptation mechanism involves changes in their lipid composition. For example, enhanced accumulation of storage lipids (TG) was observed during nitrogen stress for the marine diatom (Parrish and Wangersky, 1987), during bloom decay (Parrish, 1987) and during oligotrophication in the NW Mediterranean (Bourguet et al., 2008). Increasing oligotrophy in the northern Adriatic Sea led to an increasing number of phytoplankton taxa, enhanced lipid biosynthesis and increasing synthesis of glycolipids (MGDG), as these molecules do not contain nitrogen or phosphorus (Frka et al., 2011). Similarly, phytoplankton may overcome phosphorus deficiency by synthesis of sulfoquinovosyldiacylglycerol, a lipid with sulfur and sugar in place of phosphate (Van Mooy et al., 2006). Moreover, intensive wildfire episodes which are expected to increase in future qualitatively and quantitatively modify lipid production of surface layers in the coastal environment (Milinković et al., 2022). Therefore, we may expect that future scenarios could result in qualitative and quantitative changes of biogenic lipid pool and its accumulation and photo-transformation at the air-water interface with global consequence. This study thus clearly points toward a global impact of the biogenic lipid photochemistry at the air-sea interface, with in depth studies of the lipid remodelling, caused by environmental changes, presenting the next essential step in understanding the drivers behind the differences in their VOCs production, as well as their impacts on the atmospheric processes.

4. Conclusions

For the first time, photochemical processing at the air-water interface containing organic material from an authentic culture of the marine diatom *Chaetoceros pseudocurvisetus* was studied. Upon irradiation, the total and dissolved phytoplankton material, and in particular its isolated lipid fraction present at the air-water interface, acted as a source of abiotic production of saturated oxygenated compounds as well as unsaturated and functionalized VOCs, while OM photochemical transformation was followed by changes in surfactant activity of exposed biogenic material. Our findings confirm that particulate material from dead cells may play a role in facilitating the accumulation of biogenic surfactants at the air-water interface. The highest normalized flux intensity determined for the lipid material suggests that biogenic lipids,

as less water-soluble substances, i.e., efficient surfactants present at the air-water interface, are primarily responsible for the photochemical reactions leading to the production of VOCs from diatom OM exposed to irradiation. The VOCs fluxes determined from the lipid sample were within the range of previous field observations and laboratory experiments, suggesting that the observed processes could occur to a similar extent in the marine environment, particularly in the sea surface microlayer. It should be noted that such VOCs emissions have previously been attributed to processes driven by biology, artificial surfactants in the laboratory, and biofilm containing a mixture of different microorganisms. In contrast, the observed results suggest that VOCs released during irradiation of exclusively biogenic lipid material accumulated at the ocean-atmosphere interface might lead to similar emissions into the atmosphere. Additionally, we demonstrated that the emitted VOCs can significantly affect the oxidation potential of the atmosphere and promote aerosol formation and growth. Oxidation by dark ozonolysis and subsequent particle formation clearly demonstrate the formation and release of unsaturated VOCs. Given that marine biogenic lipids as common natural surfactants can be considered ubiquitous at air-water interfaces, such as on rivers, lakes, oceans, aerosol particles, and cloud droplets, photo-induced abiotic VOCs production can be expected to occur globally, influencing ocean-atmosphere exchange processes as well as atmospheric chemistry on a large scale.

List of abbreviations:

Volatile organic compounds (VOCs); Secondary organic aerosol (SOA); Sea surface microlayer (SML); Sterol esters (SE); Fatty acid methyl esters (ME); Fatty ketone hexadecanone (KET); Triacylglycerols (TG); Free fatty acids (FFA); Fatty alcohols (ALC); 1,3-diacylglycerols (1,3 DG); Sterols (ST); 1,2-diacylglycerols (1,2 DG); Pigments (PIG); Monoacylglycerols (MG); Glycolipids (GL): Monogalactosyldiacylglycerols (MGDG); Digalactosyldiacylglycerols (DGDG); Sulfoquinovosyldiacylglycerols (SQDG), Phospholipids (PL); Phosphatidylglycerols (PG); Phosphatidylethanolamines (PE); Phosphatidylcholine (PC). organic matter (OM); dissolved organic matter (DOM); original phytoplankton solution (TS); phytoplankton derived dissolved organic matter sample (DS); biogenic lipid material sample (LS); dissolved organic carbon (DOC); particulate organic carbon (POC); surface-active substances (SAS); chlorophyll a (Chl a); lipids in the dissolved fraction (DLip); Chromophoric dissolved organic matter (CDOM).

Acknowledgement

This research was financed by the European Union's Horizon 2020 research and innovation programme - EUROCHAMP-2020 Infrastructure Activity under grant agreement No 730997, the French-Croatian bilateral COGITO project and Croatian Science Foundation project BiREADI IP-2018-01-3105.

References

Aller, J.Y., Radway, J.C., Kilthau, W.P., Bothe, D.W., Wilson, T.W., Vaillancourt, R.D., Quinn, P.K., Coffman, D.J., Murray, B.J., Knopf, D.A., 2017. Size-resolved characterization of the polysaccharidic and proteinaceous components of sea spray aerosol, Atmos. Environ. 154, 331–347, https://doi.org/10.1016/j.atmosenv.2017.01.053.

Alpert, P.A., Kilthau, W.P., Bothe, D.W., Radway, J.C., Aller, J.Y., Knopf, D.A., 2015. The Influence of Marine Microbial Activities on Aerosol Production: A Laboratory Mesocosm Study J. Geophys. Res. Atmos. 120(17), 8841-8860.. https://doi.org/10.1002/2015JD023469.

Alpert, P.A., Ciuraru, R., Rossignol, S., Passananti, M., Tinel, L., Perrier, S., Dupart, Y., Steimer, S.S., Ammann, M., Donaldson, D.J. George, C., 2017. Fatty Acid Surfactant Photochemistry Results in New Particle Formation. Sci. Rep. 7, 1–11. https://doi.org/10.1038/s41598-017-12601-2.

Arneth, A., Monson, R.K., Schurgers, G., Niinemets, Ü., Palmer, P.I., 2008. Why are estimates of global terrestrial isoprene emissions so similar (and why is this not so for monoterpenes)? Atmos. Chem. Phys. 8, 4605–4620, https://doi.org/10.5194/acp-8-4605-2008.

Arnold, S.R., Spracklen, D.V., Williams, J., Yassaa, N., Sciare, J., Bonsang, B., Gros, V., Peeken, I., Lewis, A.C., Alvain, S., Moulin, C., 2009. Evaluation of the global oceanic isoprene source and its impacts on marine organic carbon aerosol, Atmos. Chem. Phys. 9, 1253–1262, https://doi.org/10.5194/acp-9-1253-2009.

Barthelmess, E.T., Schütte, F., Engel, A. 2021., Variability of the Sea Surface Microlayer Across a Filament's Edge and Potential Influences on Gas Exchange. Front. Mar. Sci. 8, 718384, https://doi.org/10.3389/fmars.2021.718384.

Beale, R., Dixon, J.L., Smyth, T.J., Nightingale, P.D. 2015., Annual study of oxygenated

679 volatile organic compounds in UK shelf waters. Mar. Chem. 171.
680 https://doi.org/10.1016/j.marchem.2015.02.013.
681 Bernard, F., Ciuraru, R., Boréave, A., George, C., 2016. Photosensitized formation of
682 secondary organic aerosols above the air/water interface. Environ. Sci. Technol. 50, 16,
683 8678–8686. https://doi.org/10.1021/acs.est.6b03520.
684 Bloug, N.V. 2005., Photochemistry of the sea-surface microlayer, In: Liss, P.S. and Duce, R.A.
685 (eds.), Sea surface and global change. 383–424. The United Kingdom: Cambrigde
686 University Press.
687 Booge, D., Marandino, C.A., Schlundt, C., Palmer, P.I., Schlundt, M., Atlas, E.L., Bracher, A.,
688 Saltzman, E.S., Wallace, D.W.R., 2016. Can simple models predict large-scale surface
689 ocean isoprene concentrations?, Atmos. Chem. Phys. 16, 11807–11821,
690 https://doi.org/10.5194/acp-16-11807-2016.
691 Bourguet, N., Goutx, M., Ghiglione, M., Pujo-Pay, M., Mevel, G., Momzikoff, A., Mousseau,
692 L.,Guigue, C., Garcia, N., Raimbault, P., Pete, R., Oriol, L., Lefevre, D., 2009. Lipid
693 biomarkers and bacterial lipase activities as indicators of organic matter and bacterial
694 dynamics in contrasted regimes at the Dyfamed site, NW Mediterranean, Deep-Sea Res.
695 Pt. II. 56(18) 1454-1469. https:// doi.org/10.1016/j.dsr2.2008.11.034.
696 Bryant, D.A., 2003. The beauty in small things revealed. PNAS, 100.17: 9647-9649.
697 https://doi.org/10.1073/pnas.1834558100.
698 Brüggemann, M., Hayeck, N., Bonnineau, C., Pesce, S., Alpert, P.A., Perrier, S., Zuth, C.,
699 Hoffmann, T., Chen, J., George, C., 2017. Interfacial photochemistry of biogenic
700 surfactants: A major source of abiotic volatile organic compounds. Faraday Discuss. 200,
701 59–74. https://doi.org/10.1039/c7fd00022g.
702 Brüggemann, M., Hayeck, N., George, C., 2018. Interfacial photochemistry at the ocean
703 surface is a global source of organic vapors and aerosols. Nat. Commun. 9:2101
704 https://doi.org/10.1038/s41467-018-04528-7.
705 Bruland, K.W., Rue, E.L., Smith, G.J., DiTullio, G.R., 2005. Iron, macronutrients and diatom
706 blooms in the Peru upwelling regime: brown and blue waters of Peru. Mar. Chem. 93(2-
707 4), 81-103. https://doi.org/10.1016/j.marchem.2004.06.011.
708 Buhr, K., van Ruth, S., Delahunty, C., 2002. Analysis of volatile flavour compounds by Proton
709 Transfer Reaction-Mass Spectrometry: fragmentation patterns and discrimination
710 between isobaric and isomeric compounds. Int. J. Mass Spectrom. 221(1), 1-7.
711 https://doi.org/10.1016/S1387-3806(02)00896-5.
712 Burrows, S.M., Ogunro, O., Frossard, A.A., Russell, L.M., Rasch, P.J., Elliott, S.M., 2014. A

physically based framework for modeling the organic fractionation of sea spray aerosol from bubble film Langmuir equilibria. Atmos. Chem. Phys. 14(24), 13601-13629. https://doi.org/10.5194/acpd-14-5375-2014.

Cappellin, L., Karl, T., Probst, M., Ismailova, O., Winkler, P. M., Soukoulis, C., Aprea, E., Mark, T.D. Gasperi, F., Biasioli, F., 2012. On quantitative determination of volatile organic compound concentrations using proton transfer reaction time-of-flight mass spectrometry. Environ. Sci. Technol. 46 (4), 2283-2290, https://doi.org/10.1021/es203985t.

Carslaw, N., Bell, N., Lewis, A.C., McQuaid, J.B., Pilling, M.J., 2000. A detailed case study of isoprene chemistry during the EASE96 Mace Head campaign, Atmos. Environ. 34, 2827– 2836, https://doi.org/10.1016/S1352-2310(00)00088-1.

Chhantyal-Pun, R., Rotavera, B., McGillen, M.R., Khan, M.A.H., Eskola, A.J., Caravan, R.L., Blacker, L., Tew, D.P., Osborn, D.L., Percival, C.J., Taatjes, C.A., Shallcross, D.E., Orr-Ewing, A.J., 2018. Criegee Intermediate Reactions with Carboxylic Acids: A Potential Source of Secondary Organic Aerosol in the Atmosphere. ACS Earth Space Chem. 2, 833–842. https://doi.org/10.1021/acsearthspacechem.8b00069.

Chingin, K., Yan, R.H., Zhong, D.C., Chen, H.W., 2018. Enrichment of surface-active compounds in bursting bubble aerosols. Acs Omega, 3, 8709–8717. doi: 10.1021/acsomega.8b01157.

Chiu, R., Tinel, L., Gonzalez, L., Ciuraru, R., Bernard, F., George, C., Volkamer, R., 2017. UV photochemistry of carboxylic acids at the air-sea boundary: A relevant source of glyoxal and other oxygenated VOC in the marine atmosphere. Geophys. Res. Lett. 44(2), 1079-1087. https://doi.org/10.1002/2016GL071240.

Christodoulou, S., Joux, F., Marty, J. C., Sempéré, R., Rontani, J.F., 2010. Comparative study of UV and visible light induced degradation of lipids in non-axenic senescent cells of Emiliania huxleyi. Mar. Chem. 119(1-4), 139-152.

Ciuraru, R., Fine, L., Van Pinxteren, M., D'Anna, B., Herrmann, H., George, C., 2015a. Photosensitized production of functionalized and unsaturated organic compounds at the air-sea interface. Sci. Rep., 5, 1–10. https://doi.org/10.1038/srep12741.

Ciuraru, R., Fine, L., Pinxteren, M. Van, D'Anna, B., Herrmann, H., George, C., 2015b. Unravelling New Processes at Interfaces: Photochemical Isoprene Production at the Sea Surface. Environ. Sci. Technol. 49, 13199–13205. https://doi.org/10.1021/acs.est.5b02388.

Cochran, R.E., Laskina, O., Jayarathne, T., Laskin, A., Laskin, J., Lin, P., Sultana, C., Lee, C.,

747 Moore, K.A., Cappa, C.D., Bertram, T.H., Prather, K.A., Grassian, V.H., 2016. Analysis
748 of organic anionic surfactants in fine and coarse fractions of freshly emitted sea spray
749 aerosol. Environ. Sci. Technol. 50, 2477–2486. https://doi.org/10.1021/acs.est.5b04053.
750 Conrad, A.R., Hansen, N., Jasper, A.W., Thomason, N.K., Hidaldo-Rodrigues, L., Treshock,
751 S.P., Popolan-Vaida, D.M., 2021. Identification of the acetaldehyde oxide Criegee
752 intermediate reaction network in the ozone-assisted low-temperature oxidation of: Trans
753 -2-butene. Phys. Chem. Chem. Phys. 23, 23554–23566.
754 https://doi.org/10.1039/d1cp03126k.
755 Cunliffe, M., Engel, A., Frka, S., Gašparović, B., Guitart, C., Murrell, J. C., Salter, M., Stolle,
756 C., Upstill-Goddard, R., Wurl, O., 2013. Sea surface microlayers: A unified
757 physicochemical and biological perspective of the air–ocean interface. Prog. Oceanogr.
758 109, 104-116. https://doi.org/10.1016/j.pocean.2012.08.004.
759 Ćosović, B., Vojvodić, V., 1987. Direct determination of surface active substance in natural
760 waters. Mar. Chem. 22(2-4), 363-373. https://doi.org/10.1016/0304-4203(87)90020-X.
761 Dayan, C., Fredj, E., Misztal, P.K., Gabay, M., Guenther, A.B., Tas, E., 2020. Emission of
762 biogenic volatile organic compounds from warm and oligotrophic seawater in the Eastern
763 Mediterranean. Atmos. Chem. Phys. 20, 12741–12759. https://doi.org/10.5194/acp-20-
764 12741-2020.
765 Deng, P., Wang, L., Wang, L., 2018. Mechanism of Gas-Phase Ozonolysis of β-Myrcene in
766 the Atmosphere. J. Phys. Chem. A. 122, 3013–3020.
767 https://doi.org/10.1021/acs.jpca.8b00983.
768 Dixon, J. L., Beale, R., Nightingale, P.D., 2011a. Rapid biological oxidation of methanol in
769 the tropical Atlantic: Significance as a microbial carbon source. Biogeosciences 8.
770 https://doi.org/10.5194/bg-8-2707-2011.
771 Dixon, Joanna L., Beale, R., Nightingale, P.D., 2011b. Microbial methanol uptake in northeast
772 Atlantic waters. ISME J. 5. https://doi.org/10.1038/ismej.2010.169.
773 Dixon, J.L., Beale, R., Nightingale, P.D., 2013. Production of methanol, acetaldehyde, and
774 acetone in the Atlantic Ocean. Geophys. Res. Lett. 40, 4700–4705.
775 https://doi.org/10.1002/grl.50922.
776 Duporté, G. J. Parshintsev, L.M.F. Barreira, K.M. Hartonen, M. Kulmala, Riekkola, M.-L.,
777 2016. Nitrogen-Containing Low Volatile Compounds from Pinonaldehyde-
778 Dimethylamine Reaction in the Atmosphere: A Laboratory and Field Study. Environ. Sci.
779 Technol. 50, 4693–4700. https://doi.org/10.1021/acs.est.6b00270.
780 Ehling-Schulz, M., Scherer. S., 1999. UV protection in cyanobacteria. Eur. J. Phycol. 34(4):

329-338. https://doi.org/10.1080/09670269910001736392.

Ellison, G.B., Tuck, A.F., Vaida, V., 1999. Atmospheric processing of organic aerosols, J. Geophys. Res. Atmos. 104, 11633–11641, https://doi.org/10.1029/1999JD900073.

Engel, A., Bange, H.W., Cunliffe, M., Burrows, S.M., Friedrichs, G., Galgani, L., Herrmann, H., Hertkorn, N., Johnson, M., Liss, P.S., Quinn, P.K., Schartau, M., Solovies, A., Stolle, C., Upstill-Goddard, R.C., van Pixteren, M., Zäncker, B., 2017. The ocean's vital skin: Toward an integrated understanding of the sea surface microlayer. Front. Mar. Sci. 165. https://doi.org/10.3389/fmars.2017.00165.

Facchini, M.C., Rinaldi, M., Decesari, S., Carbone, C., Finessi, E., Mircea, M., Fuzzi, S., Ceburnis, D., Flanagan, R., Nilsson, E.D., de Leeuw, G., Martino, M., Woeltjen, J., O'Dowd, C.D., 2008. Primary submicron marine aerosol dominated by insoluble organic colloids and aggregates. Geophys. Res. Lett. 35:5. https://doi.org/10.1029/2008GL034210.

Field, C.B., Behrenfeld, M.J., Randerson, J.T., Falkowski, P., 1998. Primary production of the biosphere: integrating terrestrial and oceanic components. Science, 281(5374), 237-240. https://doi.org/10.1126/science.281.5374.237.

Frew, N.M., 2005. The role of organic films in air-sea gas exchange, in The Sea Surface and Global Change, P.S. Liss and R.A. Duce (eds), pp. 121–171, Cambridge Univ. Press, U.K.

Friedman, B., Farmer, D.K., 2018. SOA and gas phase organic acid yields from the sequential photooxidation of seven monoterpenes. Atmos. Environ. 187, 335–345. https://doi.org/10.1016/j.atmosenv.2018.06.003.

Frka, S., Kozarac, K.. Ćosović, B., 2009. Characterization and seasonal variations of surface active substances in the natural sea surface microlayers of the coastal Middle Adriatic stations. Estuar. Coast. Shelf Sci. 85, 555-564. https://doi.org/10.1016/j.ecss.2009.09.023.

Frka, S., Gašparović, B., Marić, D., Godrijan, J., Djakovac, T., Vojvodić, V., Dautović, J., Kozarac, Z., 2011. Phytoplankton driven distribution of dissolved and particulate lipids in a semi-enclosed temperate sea (Mediterranean): Spring to summer situation. Estuar. Coast. Shelf Sci. 93, 290–304. https://doi.org/10.1016/j.ecss.2011.04.017.

Frka, S., Pogorzelski, S., Kozarac, Z., Ćosović, B., 2012. Physicochemical Signatures of Natural Sea Films from Middle Adriatic Stations. J. Phys. Chem. A. 116, 6552−6559 https://doi.org/10.1021/jp212430a.

Frossard, A.A., Russell, L.M., Burrows, S.M., Elliott, S.M., Bates, T.S., Quinn, P.K., 2014. Sources and composition of submicron organic mass in marine aerosol particles. J. Geophys. Res. Atmos. 119, 12977–13003. https://doi.org/10.1002/2014JD021913.

Frossard, A.A., Gerard, V., Duplessis, P., Kinsey, J.D., Lu, X., Zhu, Y., Bisgrove, J., Maben, J.R., Long, M.S., Chang, R.Y.-W., Beaupre, S.R., Kieber, D.J., Keene, W.C., Noziere, B., Cohen, R.C., 2019. Properties of seawater surfactants associated with primary marine aerosol particles produced by bursting bubbles at a model air-sea interface. Environ. Sci. Technol. 53, 9407–9417. https://doi.org/10.1021/acs.est.9b02637.

Fu, H., Ciuraru, R., Dupart, Y., Passananti, M., Tinel, L., Rossignol, S., Perrier, S., Donaldson, D.J., Chen, J., George, C., 2015. Photosensitized production of atmospherically reactive organic compounds at the air/aqueous interface. J. Am. Chem. Soc. 137(26), 8348–8351. https://doi.org/10.1021/jacs.5b04051.

Gašparović, B., Kazazić, S.P., Cvitešić, A., Penezić, A., Frka, S., 2015. Improved separation and analysis of glycolipids by Iatroscan thin-layer chromatography-flame ionization detection. J. Chromatogr. A. 1409, 259–267. https://doi.org/10.1016/j.chroma.2015.07.047.

Gašparović, B., Kazazić, S.P., Cvitešić, A., Penezić, A., Frka, S., 2017. Corrigendum to "Improved separation and analysis of glycolipids by Iatroscan thin-layer chromatography–flame ionization detection" [J. Chromatogr. A 1409 2015) 259–267](S0021967315010158)(10.1016/j.chroma.2015.07.047). J. Chromatogr. A. 1521. https://doi.org/10.1016/j.chroma.2017.09.038.

George, C., Ammann, M., D'Anna, B., Donaldson, D.J., Nizkorodov, S.A., 2015. Heterogeneous Photochemistry in the Atmosphere. Chem. Rev. 115:4218–4258. https://doi.org/10.1021/cr500648z.

Guenther, A., Karl, T., Harley, P., Wiedinmyer, C., Palmer, P.I., Geron, C., 2006. Estimates of global terrestrial isoprene emissions using MEGAN (Model of Emissions of Gases and Aerosols from Nature), Atmos. Chem. Phys. 6, 3181–3210, https://doi.org/10.5194/acp-6-3181-2006.

Guenther, A.B., Jiang, X., Heald, C.L., Sakulyanontvittaya, T., Duhl, T., Emmons, L.K., Wang, X., 2012. The Model of Emissions of Gases and Aerosols from Nature version 2.1 (MEGAN2.1): an extended and updated framework for modeling biogenic emissions, Geosci. Model Dev. 5, 1471–1492, https://doi.org/10.5194/gmd-5-1471-2012.

Guillard, R.R.L., 1975. Culture of Phytoplankton for Feeding Marine Invertebrates, in: Culture of Marine Invertebrate Animals. https://doi.org/10.1007/978-1-4615-8714-9_3

Guschina, I.A., Harwood, J.L., 2006. Lipids and lipid metabolism in eukaryotic algae. Prog. Lipid Res. 45, 160–186. https://doi.org/10.1016/j.plipres.2006.01.001.

Guschina, I.A. Harwood, J.L., 2009. Algal Lipids and Effect of the Environment on Their

Biochemistry. In: Arts, M.T., Brett, M.T., and Kainz, M., Eds., Lipids in Aquatic Ecosystems, Springer Science, Business Media LLC, 1-24. http://dx.doi.org/10.1007/978-0-387-89366-2_1.

Hammes, J., Lutz, A., Mentel, T., Faxon, C., Hallquist, M., 2018. Carboxylic acids from limonene oxidation by ozone and OH radicals: Insights into mechanisms derived using a FIGAERO-CIMS. Atmos. Chem. Phys. 1–23. https://doi.org/10.5194/acp-2018-1004

He, Y.-Y., Häder, D-P., 2002. Reactive oxygen species and UV-B: effect on cyanobacteria. Photochem. Photobiol. Sci. 1(10), 729-736. https://doi.org/10.1039/B110365M.

Heath, R.L., Packer, L., 1968. Photoperoxidation in isolated chloroplasts. II. Role of electron transfer. Arch. Biochem. Biophys. 125, 850–857, https://doi.org/10.1016/0003-9861(68)90523-7.Hu, Q.H., Xie, Z.Q., Wang, X.M., Kang, H., He, Q.F., Zhang, P., 2013. Secondary organic aerosols over oceans via oxidation of isoprene and monoterpenes from Arctic to Antarctic. Sci. Rep., 3, 2280. https://doi.org/10.1038/srep02280.

Hu, Q.H., Xie, Z.Q., Wang, X.M., Kang, H., Zhang, Y.Q., Ding, X., Zhang, P.F., 2018 Monocarboxylic and dicarboxylic acids over oceans from the East China Sea to the Arctic Ocean: Roles of ocean emissions, continental input and secondary formation. Sci. Total Environ. 640, 284–292, https://doi.org/10.1016/j.scitotenv.2018.05.311.

Huang, D., Wang, J., Xia, H., Zhang, Y., Bao, F., Li, M., Chen, C., Zhao, J., 2020. Enhanced photochemical volatile organic compounds release from fatty acids by surface-enriched Fe (III). Environ. Sci. Technol. 54(21), 13448-13457, https://doi.org/10.1021/acs.est.0c03793.

Jiang, H., Carena, L., He, Y., Wang, Y., Zhou, W., Yang, L., Luan, T., Li, X., Brigante, M., Vione, D., Gligorovski, S., 2021. Photosensitized Degradation of DMSO Initiated by PAHs at the Air-Water Interface, as an Alternative Source of Organic Sulfur Compounds to the Atmosphere. J. Geophys. Res. Atmos. 126(22), e2021JD035346, https://doi.org/10.1029/2021JD035346.

Jimenez, J.L., Canagaratna, M.R., Donahue, N.M., Prevot, A.S.H., Zhang, Q., et al. 2009. Evolution of organic aerosols in the atmosphere. Science 329(5959): 1525-1529. https://doi.org/10.1126/science.1180353.

Kalalian, C., Abis, L., Depoorter, A., Lunardelli, B., Perrier, S., George, C., 2020. Influence of indoor chemistry on the emission of mVOCs from Aspergillus niger molds. Sci. Total Environ. 741, 140148. https://doi.org/10.1016/j.scitotenv.2020.140148.

Kang, M.J., Yang, F., Ren, H., Zhao, W. Y., Zhao, Y., Li, L. J., Yan, Y., Zhang, Y.J., Lai, S. C., Zhang, Y.Y., Yang, Y., Wang, Z.F., Sun, Y.L., Fu, P.Q., 2017. Influence of continental

organic aerosols to the marine atmosphere over the East China Sea: Insights from lipids, PAHs and phthalates, Sci. Total Environ. 607, 339–350, https://doi.org/10.1016/j.scitotenv.2017.06.214.

Kameyama, S., Yoshida, S., Tanimoto, H., Inomata, S., Suzuki, K. Yoshikawa-Inoue, H., 2014. High-resolution observations of dissolved isoprene in surface seawater in the Southern Ocean during austral summer 2010-2011. J. Oceanogr. 70, 225–239. https://doi.org/10.1007/s10872-014-0226-8.

Keller, M.D., Bellows, W.K., Guillard, R.R., 1988. Microwave treatment for sterilization of phytoplankton culture media. J. Exp. Mar. Biol. Ecol. 117(3), 279-283. https://doi.org/10.1016/0022-0981(88)90063-9.

Kieber, R.J., Hydro, L.H., Seaton, P.J., 1997. Photooxidation of triglycerides and fatty acids in seawater: Implication toward the formation of marine humic substances. Limnol. Oceanogr. 42, 1454–1462. https://doi.org/10.4319/lo.1997.42.6.1454.

Kozarac, Z., Ćosović, B., Möbius, D., Dobrić, M., 2000. Interaction of Polysaccharides with Lipid Monolayers, J. Colloid Interface Sci. 226 (2) 210-217, https://doi.org/10.1006/jcis.2000.6839.

Kroflič, A., Frka, S., Simmel, M., Wex, H., Grgić, I., 2018. Size-resolved surface-active substances of atmospheric aerosol: Reconsideration of the impact on cloud droplet formation. Environ. Sci. Technol. 52(16), 9179-9187. https://doi.org/10.1021/acs.est.8b02381.

Kuznetsova, M., Lee, C., 2002. Dissolved free and combined amino acids in nearshore surface microlayers: influence of extracellular hydrolysis. Aquat. Sci. 64, 252– 268. https://doi.org/10.1007/s00027-002-8070-0.

Kuznetsova, M., Lee, C., Aller, J., 2005. Characterization of the proteinaceous matter in marine aerosols, Mar. Chem. 96, 359–377, https://doi.org/10.1016/j.marchem.2005.03.007.

Levitan, O., Dinamarca, J., Hochman, G., Falkowski, P.G., 2014. Diatoms: a fossil fuel of the future. Trends Biotechnol. 32(3), pp.117-124. https://doi.org/10.1016/j.tibtech.2014.01.004.

Levitan, O., Dinamarca, J., Zelzion, E., Lun, D. S., Guerra, L.T., Kim, M.K., Kim, J., Van Mooy, B.A.S., Bhattacharya, D., Falkowski, P.G., 2015. Remodeling of intermediate metabolism in the diatom Phaeodactylum tricornutum under nitrogen stress. PNAS, 112(2), 412-417. https://doi.org/10.1073/pnas.1419818112.

Lewis, A.C., Hopkins, J.R., Carpenter, L.J., Stanton, J., Read, K.A., Pilling, M.J., 2005. Sources and sinks of acetone, methanol, and acetaldehyde in North Atlantic marine air.

Atmos. Chem. Phys. 5, 1963–1974. https://doi.org/10.5194/acp-5-1963-2005.

Luo, G., Yu, F., 2010. A numerical evaluation of global oceanic emissions of α-pinene and isoprene. Atmos. Chem. Phys. 9. https://doi.org/10.5194/acp-10-2007-2010.

Malviya, S., Scalco, E., Audic, S., Vincent, F., Veluchamy, A., Poulain, J., Wincker, P., Iudicone, D., De Vargas, C., Bittner, L., Zingone, A., Bowler, C., 2016. Insights into global diatom distribution and diversity in the world's ocean. PNAS, 113, E1516–E1525. https://doi.org/10.1073/pnas.1509523113.

Marić, D., Frka, S., Godrijan, J., Tomažić, I., Penezić, A., Djakovac, T., Vojvodić, V., Precali, R., Gašparović, B., 2013. Organic matter production during late summer-winter period in a temperate sea. Cont. Shelf Res. 55. https://doi.org/10.1016/j.csr.2013.01.008

Marmulla, R., Harder, J., 2014. Microbial monoterpene transformations-a review. Front. Microbiol. 5, 1–14. https://doi.org/10.3389/fmicb.2014.00346.

Marty, J.C., Saliot, A., Buatmenard, P., Chesselet, R., Hunter, K.A., 1979. Relationship between the lipid compositions of marine aerosols, the sea surface microlayer, and subsurface water, J. Geophys. Res. Oceans. 84, 5707–5716, https://doi.org/10.1029/JC084iC09p05707.

Marty, J.C., Žutić, V., Precali, R., Saliot, A., Ćosović, B., Smodlaka, N., Cauwet, G., 1988. Organic matter characterization in the Northern Adriatic Sea with special reference to the sea surface microlayer. Mar. Chem. 25(3), 243-263. https://doi.org/10.1016/0304-4203(88)90053-9.

Mekic, M., Zeng, J., Jiang, B., Li, X., Lazarou, Y. G., Brigante, M., Herrmann, H., Gligorovski, S., 2020. Formation of toxic unsaturated multifunctional and organosulfur compounds from the photosensitized processing of fluorene and DMSO at the air - water interface. J. Geophys. Res. Atmos., 125(6), e2019JD031839, https://doi.org/10.1029/2019JD031839.

Milinković, A., Penezić, A., Kušan, A.C., Gluščić, V., Žužul, S., Skejić, S., Šantić, D., Godec, R., Pehnec, G., Omanović, D., Engel, A., Frka, S., 2022. Variabilities of biochemical properties of the sea surface microlayer: Insights to the atmospheric deposition impacts. Sci. Total Environ. 156440. https://doi.org/10.1016/j.scitotenv.2022.156440.

Millet, D.B., Jacob, D.J., Custer, T.G., De Gouw, J.A., Goldstein, A.H., Karl, T., Singh, H.B., Sive, B.C., Talbot, R.W., Warneke, C., Williams, J., 2008. New constraints on terrestrial and oceanic sources of atmospheric methanol. Atmos. Chem. Phys. 8. https://doi.org/10.5194/acp-8-6887-2008.

Millet, D.B., Guenther, A., Siegel, D., Nelson, N., Singh, H., De Gouw, J., Warneke, C., Williams, J., Eerdekens, G., Sinha, V., Karl, T., Flocke, F., Apel, E., Riemer, D.D.,

Palmer, P.I., Barkley, M., 2010. Global atmospheric budget of acetaldehyde: 3-D model analysis and constraints from in-situ and satellite observations. Atmos. Chem. Phys. 10, 3405–3425. https://doi.org/10.5194/acp-10-3405-2010.

Mincer, T.J., Aicher, A.C., 2016. Methanol production by a broad phylogenetic array of marine phytoplankton. PLoS One, 11. https://doi.org/10.1371/journal.pone.0150820.

Mock, T., Medlin, L.K., 2012. Genomics and Genetics of Diatoms, in Advances in Botanical Research, Piganeau, G. (Ed.), 64, 245-284, Academic Press, Cambridge, Massachusetts

Mopper, K., Stahovec, W.L., 1986. Sources and sinks of low molecular weight organic carbonyl compounds in seawater. Mar. Chem. 19, 305–321. https://doi.org/10.1016/0304-4203(86)90052-6.

Mungall, E.L., Abbatt, J.P.D., Wentzell, J.J.B., Lee, A.K.Y., Thomas, J.L., Blais, M., Gosselin, M., Miller, L.A., Papakyriaoku, T., Willis, M.D., 2017. Microlayer source of oxygenated volatile organic compounds in the summertime marine Arctic boundary layer. PNAS. 114, 6203–6208. https://doi.org/10.1073/pnas.1620571114.

Nelson, J.R., 1993. Rates and possible mechanism of light-dependent degradation of pigments in detritus derived from phytoplankton. J. Mar. Res. 51(1), 155-179. https://doi.org/10.1357/0022240933223837.

Novak, T., Godrijan, J., Pfannkuchen, D.M., Djakovac, T., Mlakar, M., Baricevic, A., Tanković, M.S., Gašparović, B., 2018. Enhanced dissolved lipid production as a response to the sea surface warming. J Mar Syst. 180, 289–298. https://doi.org/10.1016/j.jmarsys.2018.01.006.

Novak, T., Godrijan, J., Pfannkuchen, D.M., Djakovac, T., Medić, N., Ivančić, I., Mlakar, M., Gašparović, B., 2019. Global warming and oligotrophication lead to increased lipid production in marine phytoplankton. Sci. Total Environ. 668, 171–183. https://doi.org/10.1016/j.scitotenv.2019.02.372.

Orellana, M. ., Matrai, P.A., Leck, C., Rauschenberg, C.D., Lee, A.M., Coz, E., 2011. Marine microgels as a source of cloud condensation nuclei in the high Arctic, PNAS, 108,13612–13617, https://doi.org/10.1073/pnas.1102457108.

Palmer, P.I., Shaw, S.L., 2005. Quantifying global marine isoprene fluxes using MODIS chlorophyll observations, Geophys. Res. Lett. 32, 9805, https://doi.org/10.1029/2005GL022592.

Parrish, C.C., 1987. Time series of particulate and dissolved lipid classes during spring phytoplankton blooms in Bedford Basin, a marine inlet. Mar. Ecol. Prog. Ser. 35, 129-139. https://doi.org/10.3354/meps035129.

985 Parrish, C.C., Wangersky, P.J., 1987. Particulate and Dissolved lipid classes in cultures of
986 Phaeodactylum tricornutum grown in cage culture turbidostats with a range of nitrogen
987 supply rates. Mar. Ecol. Prog. Ser. 35, 119–128. https://doi.org/10.3354/meps035119.
988 Penezić, A., Gašparović, B., Burić, Z., Frka, S. 2010. Distribution of marine lipid classes in
989 salty Rogoznica Lake (Croatia). Estuar. Coast. Shelf Sci. 86.
990 https://doi.org/10.1016/j.ecss.2009.11.030.
991 Pereira, R., Schneider-Zapp, K., Upstill-Goddard, R., 2016. Surfactant control of gas transfer
992 velocity along an offshore coastal transect: results from a laboratory gas exchange tank,
993 Biogeosciences, 13, 3981–3989. https://doi.org/10.5194/bg-13-3981-2016.
994 Pereira, R., Ashton, I., Sabbaghzadeh, B., Shutler, J.D., Upstill-Goddard, R.C., 2018. Reduced
995 air–sea CO_2 exchange in the Atlantic Ocean due to biological surfactants. Nat. Geosci.
996 11(7): 492-496. https://doi.org/10.1038/s41561-018-0136-2.
997 Qiu, C., Zhang, R., 2013. Multiphase chemistry of atmospheric amines. Phys. Chem. Chem.
998 Phys. 15(16), 5738-5752. https://doi.org/10.1039/C3CP43446J.
999 Quesada, A., Vincent, W.E., 1997. Strategies of adaptation by Antarctic cyanobacteria to
1000 ultraviolet radiation. Eur. J. Phycol. 32, 335-342
1001 https://doi.org/10.1080/09670269710001737269.
1002 Rontani, J.-F., Belt, S.T., 2020. Photo-and autoxidation of unsaturated algal lipids in the marine
1003 environment: An overview of processes, their potential tracers, and limitations. Org.
1004 Geochem., 139, 103941, https://doi.org/10.1016/j.orggeochem.2019.103941.
1005 Rontani, J.-F., 2011. Visible light-dependent degradation of lipidic phytoplanktonic
1006 components during senescence: a review. Phytochemistry, 58, 187-202.
1007 https://doi.org/10.1016/S0031-9422(01)00202-3.
1008 Rossignol, S., Tinel, L., Bianco, A., Passananti, M., Brigante, M., Donaldson, D.J., George, C.,
1009 2016. Atmospheric photochemistry at a fatty acid–coated air-water interface. Science, 353
1010 (6300), 699–702. https://doi.org/10.1126/science.aaf3617.
1011 Salter, M.E., Upstill-Goddard, R.C., Nightingale, P.D., Archer, S.D., Blomquist, B., Ho, D.T.,
1012 Huebert, B., Schlosser, P., Yang, M., 2011. Impact of an artificial surfactant release on
1013 air-sea gas fluxes during Deep Ocean Gas Exchange Experiment II. J. Geophys. Res.
1014 Oceans. 116(C11). https://doi.org/10.1029/2011JC007023.
1015 Shaw, S.L., Gantt, B., Meskhidze, N., 2010. Production and Emissions of Marine Isoprene and
1016 Monoterpenes: A Review. Adv. Meteorol. 2010, 408696, 1−24.
1017 https://doi.org/10.1155/2010/408696.
1018 Singh, H.B., Hara, D.O., Herlth, D., Sachse, W., Blake, D.R., Bradshaw, J.D., Kanakidou, M.,

Crutzen, P.J., 1994. Acetone in the atmosphere : Distribution , sources , and sinks. J. Geophys. Res. Atmos. 99 (D1), 1805-1819. https://doi.org/10.1029/93JD00764

Singh, H.B., Kanakidou, M., Crutzen, P.J., Jacob, D.J., 1995. High concentrations and photochemical fate of oxygenated hydrocarbons in the global troposphere. Nature 378. https://doi.org/10.1038/378050a0.

Slowey, J.F., Jeffrey, L.M., Hood, D.W., 1962. The fatty-acid content of ocean water, Geochim. Cosmochim. Acta. 26, 607–616, https://doi.org/10.1016/0016-7037(62)90041-8.

Spracklen, D.V., Arnold, S.R., Sciare, J., Carslaw, K.S., Pio, C. 2008. Globally significant oceanic source of organic carbon aerosol: global marine OC source. Geophys. Res. Lett. 35 (12). https://doi.org/10.1029/2008GL033359.

Stonik, V., Stonik, I., 2015. Low-molecular-weight metabolites from diatoms: structures, biological roles and biosynthesis. Mar. Drugs, 13, 3672–3709. https://doi.org/10.3390/md13063672.

Tang, X.D., Price, E., Praske, S.A., Lee, M.A., Shattuck, K., Purvis-Roberts, P.J., Silva, A. Asa-Awuku, Cocker, D.R., 2013. NO3 radical, OH radical and O-3-initiated secondary aerosol formation from aliphatic amines. Atmos. Environ. 2013, 72, 105–112.

Triesch, N., Van Pinxteren, M., Frka, S., Stolle, C., Spranger, T., Hans Hoffmann, E., Gong, X., Wex, H., Schulz-Bull, D., Gašparović, B., Herrmann, H., 2021. Concerted measurements of lipids in seawater and on submicrometer aerosol particles at the Cabo Verde islands: Biogenic sources, selective transfer and high enrichments. Atmos. Chem. Phys. 21, 4267–4283. https://doi.org/10.5194/acp-21-4267-2021.

Van Mooy B.A., Rocap G., Fredricks H.F., Evans C.T., Devol A.H., 2006. Sulfolipids dramatically decrease phosphorus demand by picocyanobacteria in oligotrophic marine environments. PNAS. 103(23):8607-12. https://doi.org/10.1073/pnas.0600540103.

Van Vleet, E.S., Williams, P.M., 1983. Surface potential and film pressure measurements in seawater systems 1. Limnol. Oceanogr. 28(3), 401-414. https://doi.org/10.4319/lo.1983.28.3.0401.

Warneke, C., De Gouw, J.A., Kuster, W.C., Goldan, P.D., Fall, R., 2003. Validation of atmospheric VOC measurements by proton-transfer-reaction mass spectrometry using a gas-chromatographic preseparation method. Environ. Sci. Technol. 37(11), 2494-2501. https://doi.org/10.1021/es026266i.

Wegener, R., Brauers, T., Koppmann, R., Bares, S.R., Rohrer, F., Tillman, R., Wahner, A., Hansel, A., Wisthaler, A., 2007. Simulation chamber investigation of the reactions of

ozone with short-chained alkenes. J. Geophys. Res. Atmos. 112, 1–17. https://doi.org/10.1029/2006JD007531.

Wu, S.P., Schwab, J., Liu, B.L., Li, T.C., Yuan, C.S., 2015. Seasonal variations and source identification of selected organic acids associated with PM10 in the coastal area of Southeastern China, Atmos. Res. 155, 37–51, https://doi.org/10.1016/j.atmosres.2014.11.014.

Wurl, O., Holmes, M., 2008. The gelatinous nature of the sea-surface microlayer. Mar. Chem. 110(1-2), 89-97. https://doi.org/10.1016/j.marchem.2008.02.009

Wurl, O., Wurl, E., Miller, L., Johnson, K., Vagle, S., 2011. Formation and global distribution of sea-surface microlayers. Biogeosciences, 8(1), 121-135. https://doi.org/10.5194/bg-8-121-2011.

Wurl, O., Ekau, W., Landing, W.M., Zappa, C.J., Bowman, J., 2017. Sea surface microlayer in a changing ocean–A perspective. Elementa: Science of the Anthropocene, 5. https://doi.org/10.1525/elementa.228.

Yoshimura, K., Ogawa, T. Hama, T., 2009. Degradation and dissolution properties of photosynthetically-produced phytoplankton lipid materials in early diagenesis. Mar. Chem. 114, 11–18. https://doi.org/10.1016/j.marchem.2009.03.002.

Yi, Z., Xu, M., Di, X., Brynjolfsson, S., Fu, W., 2017. Exploring valuable lipids in diatoms. Front. Mar. Sci. 4, 17. https://doi.org/10.3389/fmars.2017.00017.

Yu, Z., 2018. Chamber study of biogenic volatile organic compounds: plant emission, oxidation products and their OH reactivity. Forschungszentrum Jülich GmbH Zentralbibliothek, Verlag Jülich ISBN: 978-3-95806-356-3.

Yu, Z., Li, Y., 2021. Marine volatile organic compounds and their impacts on marine aerosol—A review. Sci. Total Environ. 768, 145054. https://doi.org/10.1016/j.scitotenv.2021.145054.

Zhou, S., Gonzalez, L., Leithead, A., Finewax, Z., Thalman, R., Vlasenko, A., Vagle, S., Miller, L.A., Li, S.M., Bureekul, S., Furutani, H., Uematsu, M., Volkamer, R., Abbatt, J., 2014. Formation of gas-phase carbonyls from heterogeneous oxidation of polyunsaturated fatty acids at the air-water interface and of the sea surface microlayer. Atmos. Chem. Phys. 14, 1371–1384. https://doi.org/10.5194/acp-14-1371-2014.

Zhou, X., Mopper, K., 1997. Photochemical production of low-molecular-weight carbonyl compounds in seawater and surface microlayer and their air-sea exchange. Mar. Chem. 56, 201–213. https://doi.org/10.1016/S0304-420396)00076-X.

Zuo, Z., 2019. Why algae release volatile organic compounds—the emission and roles. Front.

Microbiol. 10, 491. https://doi.org/10.3389/fmicb.2019.00491.

Zhu, J., Penner, J.E., Lin, G., Zhou, C., Xu, L., Zhuang, B., 2017. Mechanism of SOA formation determines magnitude of radiative effects. PNAS. 114(48), 12685-12690.

Supplemental Material for

Interfacial photochemistry of marine diatom lipids: Abiotic production of volatile organic compounds and new particle formation

Abra Penezić*[1], Xinke Wang[2,3], Sebastien Perrier[2], Christian George[2], Sanja Frka*[1]

[1]Division for Marine and Environmental Research, Ruđer Bošković Institute, Zagreb, Croatia

[2]Université Lyon, Université Claude Bernard Lyon 1 CNRS, IRCELYON, Villeurbanne, France

[3]Now at Department of Chemistry, University of California, Irvine, CA 92697-2025

*Corresponding authors: **abra@irb.hr**; **frka@irb.hr**

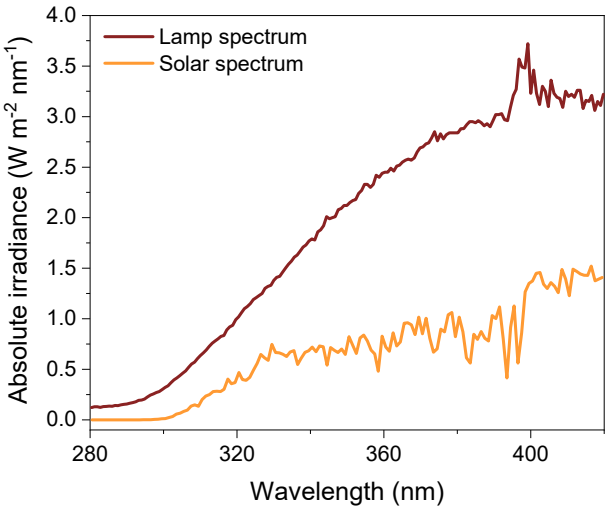

Figure S1. Absolute irradiance as function of wavelength for the actinic solar spectrum (calculated using the Tropospheric Ultraviolet and Visible (TUV) Radiation Model version 5.2; http://cprm.acom.ucar.edu/Models/TUV/Interactive_TUV) and the xenon lamp with Pyrex filter used for irradiation experiments.

Table S1. Molecular formulas of volatile organic compounds (VOCs) detected prior to the atmospheric simulation chamber experiment.

(*m/z*)	Assigned molecular formula
31.017	CH_2O
47.012	CH_2O_2
46.028	CH_3NO
33.033	CH_4O
43.017	C_2H_2O
42.033	C_2H_3N
44.012	C_2H_3O
45.033	C_2H_4O
61.027	$C_2H_4O_2$
60.050	C_2H_5NO
41.038	C_3H_4
57.033	C_3H_4O
73.027	$C_3H_4O_2$
59.047	C_3H_6O
75.042	$C_3H_6O_2$
101.020	$C_4H_4O_3$
57.068	C_4H_8
73.063	C_4H_8O
69.069	C_5H_8
101.054	$C_5H_8O_2$
101.092	$C_6H_{12}O$

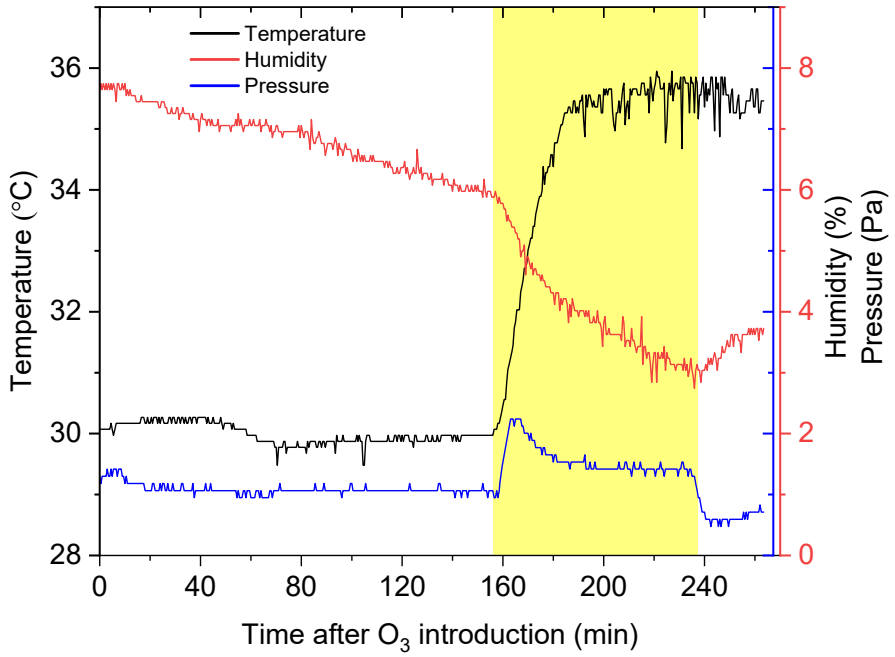

Figure S2. Temperature, humidity and pressure data inside the multiphase atmospheric simulation chamber. Irradiation period is indicated by yellow shading.

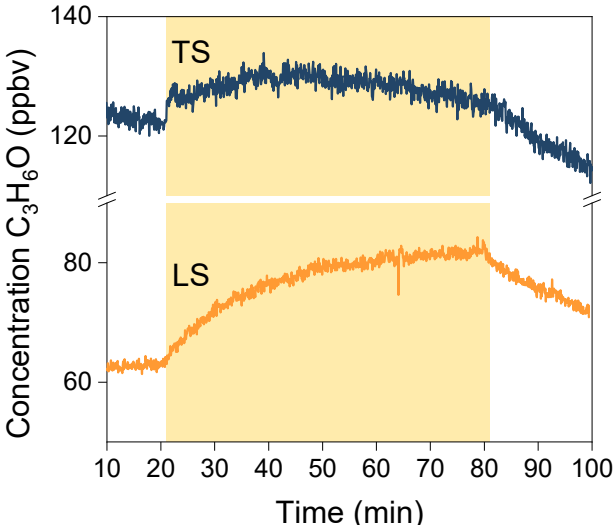

Figure S3. C_3H_6O originating from TS (original non-filtered phytoplankton solution) and LS (biogenic lipid material). Yellow colour represents the irradiation period.

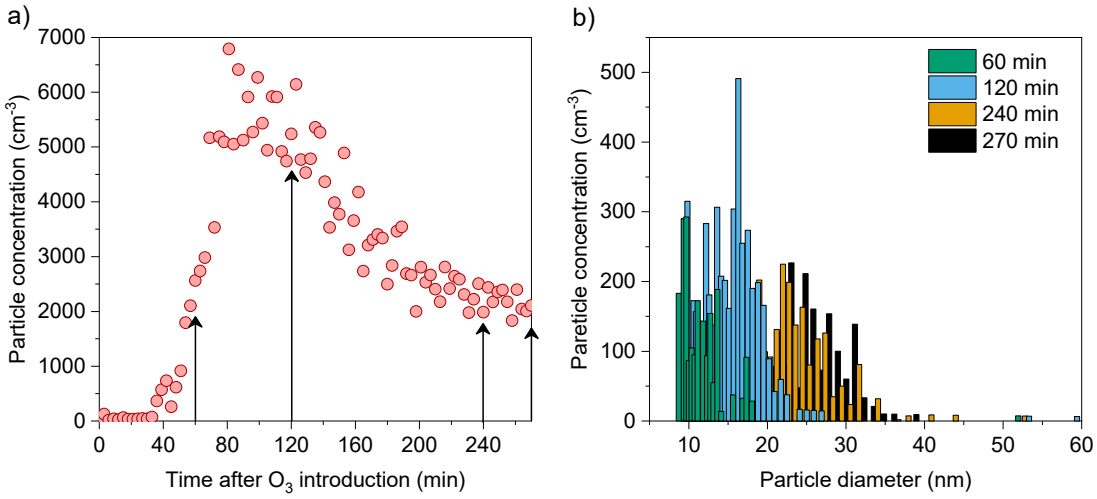

Figure S4. Total concentration of particles formed within the multiphase atmospheric simulation chamber (a) and their diameters at certain times during the experiment (60 min, 120 min, 240 min and 270 min) (b) as indicated by arrows in figure (a).